

1 **Supplementary Information: Spatial variability of VOCs, ozone, and**
2 **carbonaceous aerosols during the 2022 European summer heatwave**

3 Wenche Aas et al

4
5 **Table S1 Sites participating in the intensive measurement campaign (IMP) from 12 to 29 July, 2022.**

code	Name	latitude	longitude	altitude	Landuse
AT0002R	Illmitz	47.7667	16.7667	117.0 m	Grassland
BE0007R	TMNT09 Vielsalm	50.3040	6.0013	496.0 m	Forest
CH0010U	Zürich-Kaserne	47.3776	8.5304	409.0 m	Urban, residential
CH0053R	Beromünster	47.1896	8.1754	797.0 m	Agricultural
CY0002R	Agia Marina Xyliatou (CAO)	35.0381	33.0578	520.0 m	Agricultural
CZ0003R	Kosetice (NAOK)	49.5734	15.0803	535.0 m	Agricultural
DE0007R	Neuglobsow	53.1413	13.0317	62.0 m	Forest, park
DE0008R	Schmücke	50.6500	10.7667	937.0 m	Forest
DE0043G	Hohenpeißenberg	47.8015	11.0096	975.0 m	Grassland
DE0044R	Melpitz	51.5255	12.9277	86.0 m	Agricultural
ES0019U	Barcelona (Palau Reial)	41.3875	2.1153	80.0 m	Urban park
ES0021U	Madrid (CIEMAT)	40.4564	-3.7256	669.0 m	Urban background
ES0025U	Bilbao, María Díaz de Haro	43.2588	-2.9456	911.0 m	Urban, residential
ES1778R	Montseny	41.7667	2.3500	700.0 m	Mountain, grass/forest
FI0050R	Hyytiälä	61.8500	24.2833	181.0 m	Forest
FR0008R	Donon	48.5000	7.1333	775.0 m	Forest
FR0013R	Peyrusse Vieille	43.6167	0.1833	200.0 m	Agricultural
FR0018R	La Coulonche	48.6333	-0.4500	309.0 m	Agricultural, Forest
FR0020R	SIRTA ARO	48.7089	2.1487	162.0 m	Suburban, Agricultural
FR0022R	Obs. Perenne de l'Environ.	48.5622	5.5056	392.0 m	Agricultural
FR0027U	ATOLL (Villeneuve d'Ascq)	50.6110	3.1404	70.0 m	Suburban, residential
FR0030R	Puy de Dôme	45.7722	2.9649	1465.0 m	Mountain, forest
FR0035U	Marseille Longchamp	43.3053	5.3947	73.0 m	Urban park
FR0038U	Grenoble Frenes	45.1619	5.7356	214.0 m	Urban park
FR0041U	Paris Chatelet	48.8621	2.3446	35.0 m	Urban park
GB0048R	Auchencorth Moss	55.7922	-3.2429	260.0 m	Agricultural
GB1055R	Chilbolton Observatory	51.1496	-1.4382	78.0 m	Agricultural
IE0031R	Mace Head	53.3258	-9.8994	5.0 m	Coastal, grassland
IT0004R	Ispira	45.8146	8.6357	209.0 m	Residential background
IT0009R	Monte Cimone	44.1932	10.7014	2165.0 m	Mountain, remote park
NO0002R	Birkenes II	58.3885	8.2520	219.0 m	Forest

6
7

8 **Table S2 Overview of the different components measured during the intensive measurement campaign (IMP), 12 to 29 July, 2022.**

O-VOCs	NMHC (C2-C6)	Terpenes	Tracers	Organic_acid
2-methylpropenal	2-2-dimethylbutane	monoterpenes	3-MBTCA	2-ketobutyric_acid
2-oxopropanal	2-3-dimethylbutane		sum_2-methyltetrols	3-hydroxybutyric_acid
3-buten-2-one	2-methylbutane	3-carene	adonitol	4-hydroxybenzoic_acid
butanal	2-methylpentane	alpha-pinene	arabitol	4-methylphthalic_acid
butanone	2-methylpropane	beta-pinene	fructose	4-oxoheptanoic_acid
ethanal	3-methylpentane	camphene	glucose	adipic_acid
ethanedial	ethane	eucalyptol	inositol	azelaic_acid
methanal	ethene	limonene	lactose	benzoic_acid
propanal	ethyne	myrcene	maltose	caproic_acid
propanone	n-butane	p-cymene	mannitol	cis-pinonic_acid
	n-hexane	sabinene	mannose	citraconic_acid
	n-pentane	terpinolene	melezitose	citric_acid
	propane		rhamnose	gluconic_acid
Aromatics	propene	alpha-humulene	sorbitol	glutaric_acid
1-2-3-trimethylbenzene	propyne	beta-caryophyllene	sucrose	glycolic_acid
1-2-4-trimethylbenzene	1-3-butadiene	beta-farnesene	levoglucosan	glyoxylic_acid
1-3-5-trimethylbenzene	butenes	iso-longifolene		lactic_acid
1-ethyl-3-methylbenzene	isohexanes	longicyclene		maleic_acid
1-ethyl-4-methylbenzene	isoprene		Inorganic	malic_acid
benzene	pentenes		ammonium	malonic_acid
ethylbenzene	1-butene		calcium	methanesulfonic_acid
m-p-xylene	2-methylpropene	NMHC (C7-C12)	chloride	oxalic_acid
o-xylene	cis-2-butene	n-decane	magnesium	phthalic_acid
styrene	trans-2-butene	n-dodecane	nitrate	pimelic_acid
toluene	1-hexene	n-nonane	potassium	pinic_acid
trimethylbenzene	1-pentene	n-octane	sodium	pyruvic_acid
	2-2-dimethylpropane	n-undecane	sulphate_total	sebacic_acid
		isoheptanes	nitrogen_dioxide	suberic_acid
		2-2-4-trimethylpentane	ozone	succinic_acid
		2-3-dimethylpentane	elemental_carbon	tartaric_acid
		2-methylhexane	organic_carbon	
		3-methylheptane	pm25_mass	
		methyl-cyclohexane	pm10_mass	
		n-heptane		
		2-3-4-trimethylpentane		
		2-methylheptane		
		3-methylhexane		

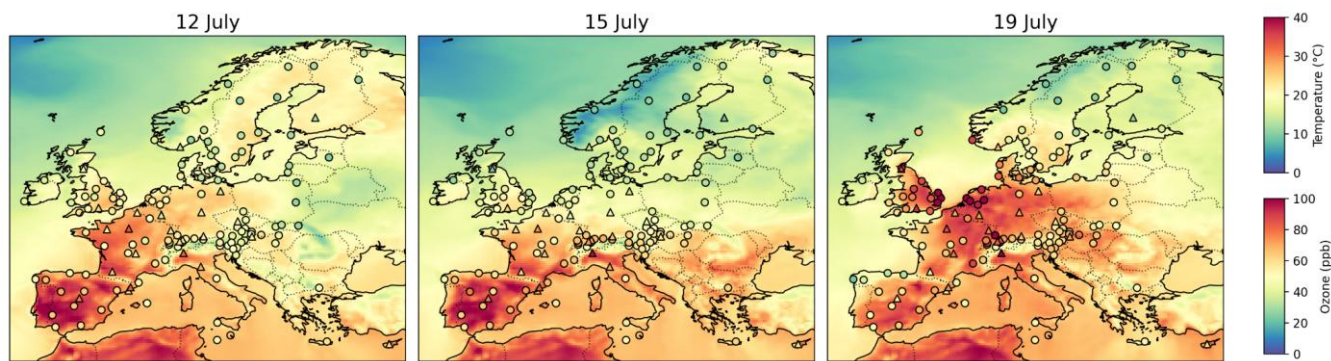


Figure S1. ERA5 (Hersbach et al., 2023) modelled average temperature between 12-16 UTC superimposed with observed maximum ozone concentration (marker color scale) for 12, 15 and 19 July 2022. The sites participating in the campaign are marked as triangles, and regular EMEP sites with circles, EMEP data from (Hjellbrekke and Solberg, 2024).

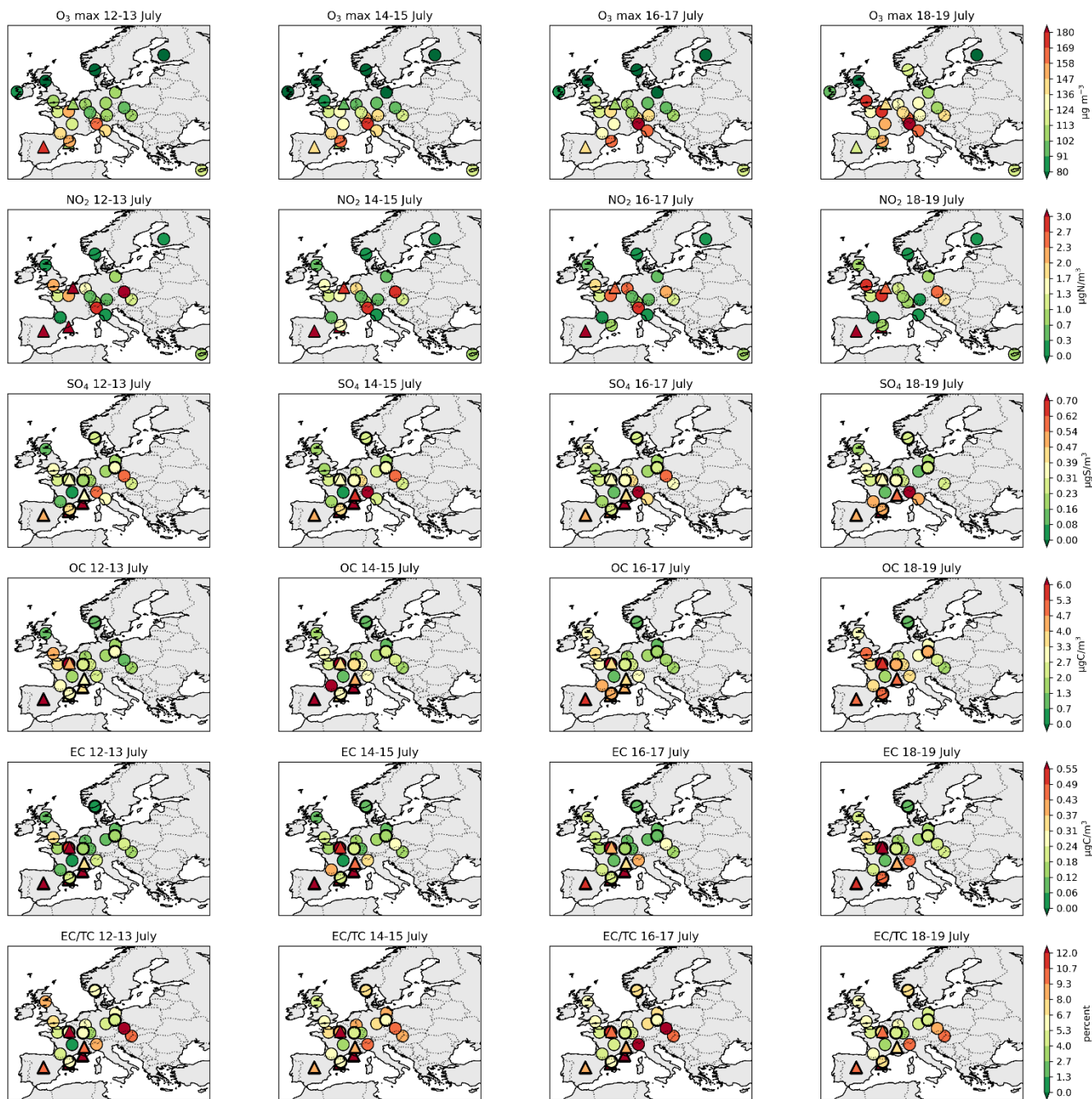


Figure S2. Spatial and temporal variations in the maximum ozone concentration, nitrogen dioxide, sulfate and organic and elemental carbon in aerosols during 12-19 July 2022. Urban sites are denoted with a triangle. Sites with a PM₁₀ size cut-off are marked with a thicker border than those with a PM_{2.5} cut-off.

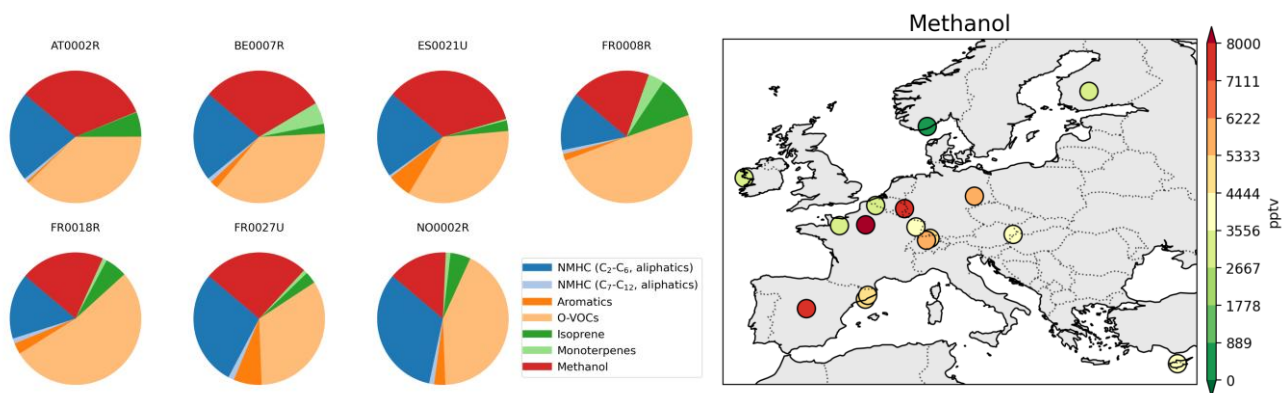


Figure S3. Distribution of different VOC groups, including methanol (left) and spatial distribution of mid-day average concentrations (right), 12-19 July 2022 .

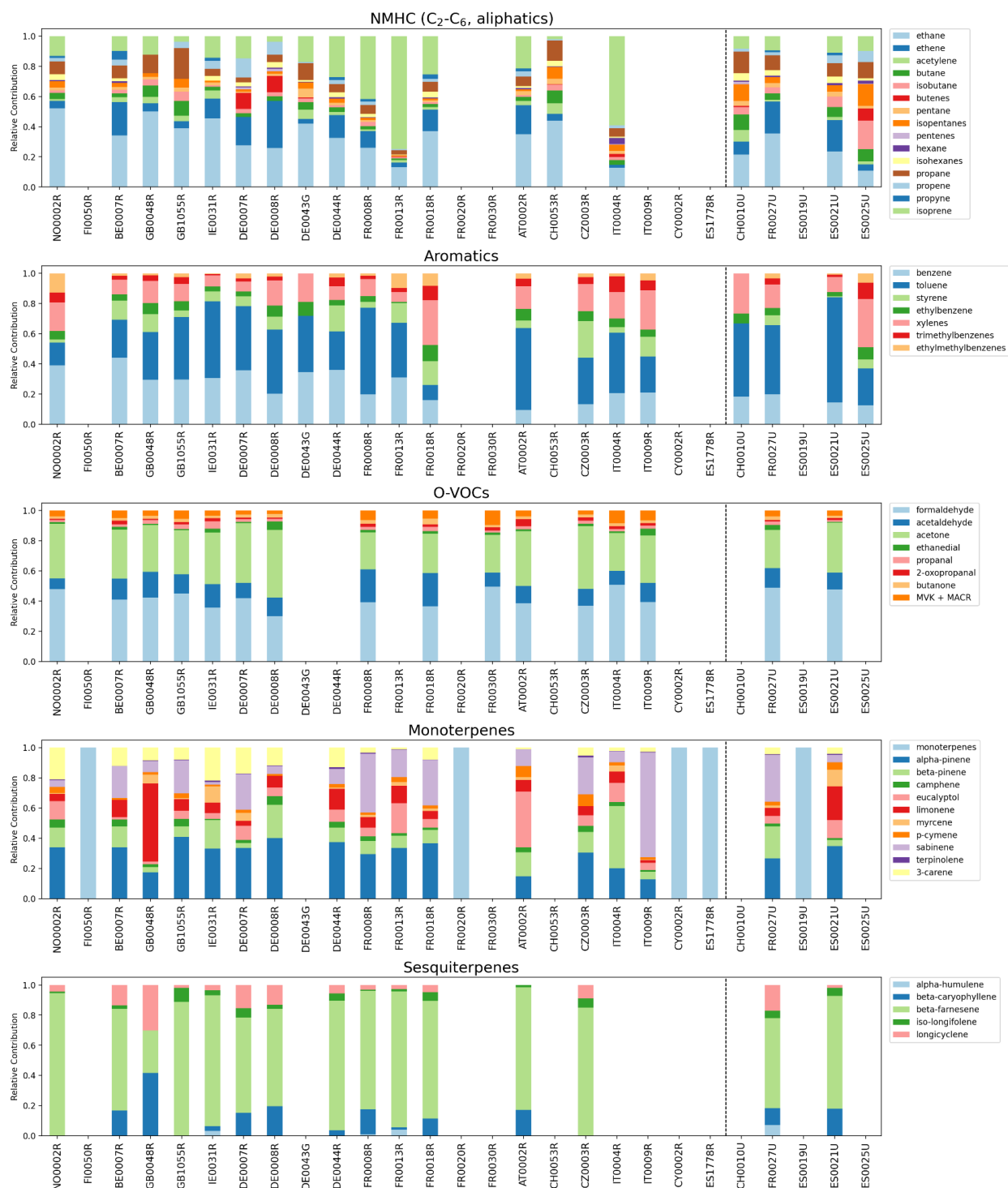
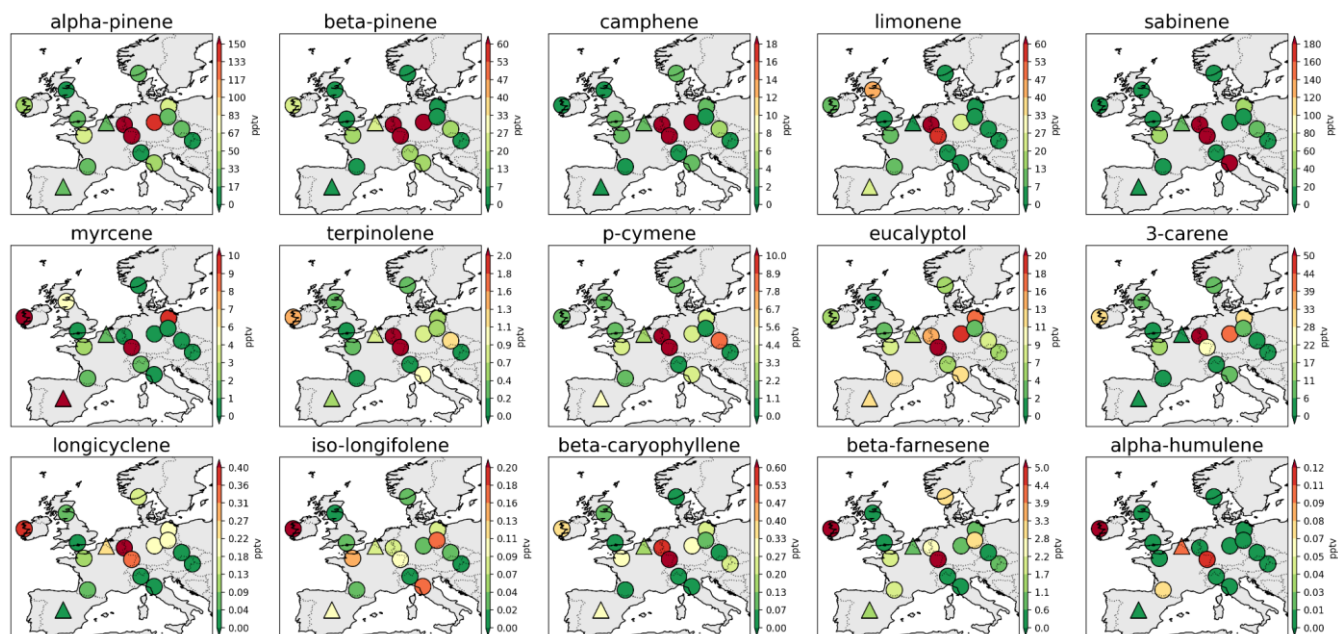


Figure S4. The relative chemical composition of the different VOC groups at all the sites, averaged over the measurement period (12-19 July 2022). The sites are sorted from north to south, with the urban sites separated to the right.

27

28



29

30

31

Figure S5. Spatial distribution of the average concentration of the different monoterpenes and sesquiterpenes analysed over the measurement period (12-19 July 2022). Urban sites are denoted with a triangle.

32

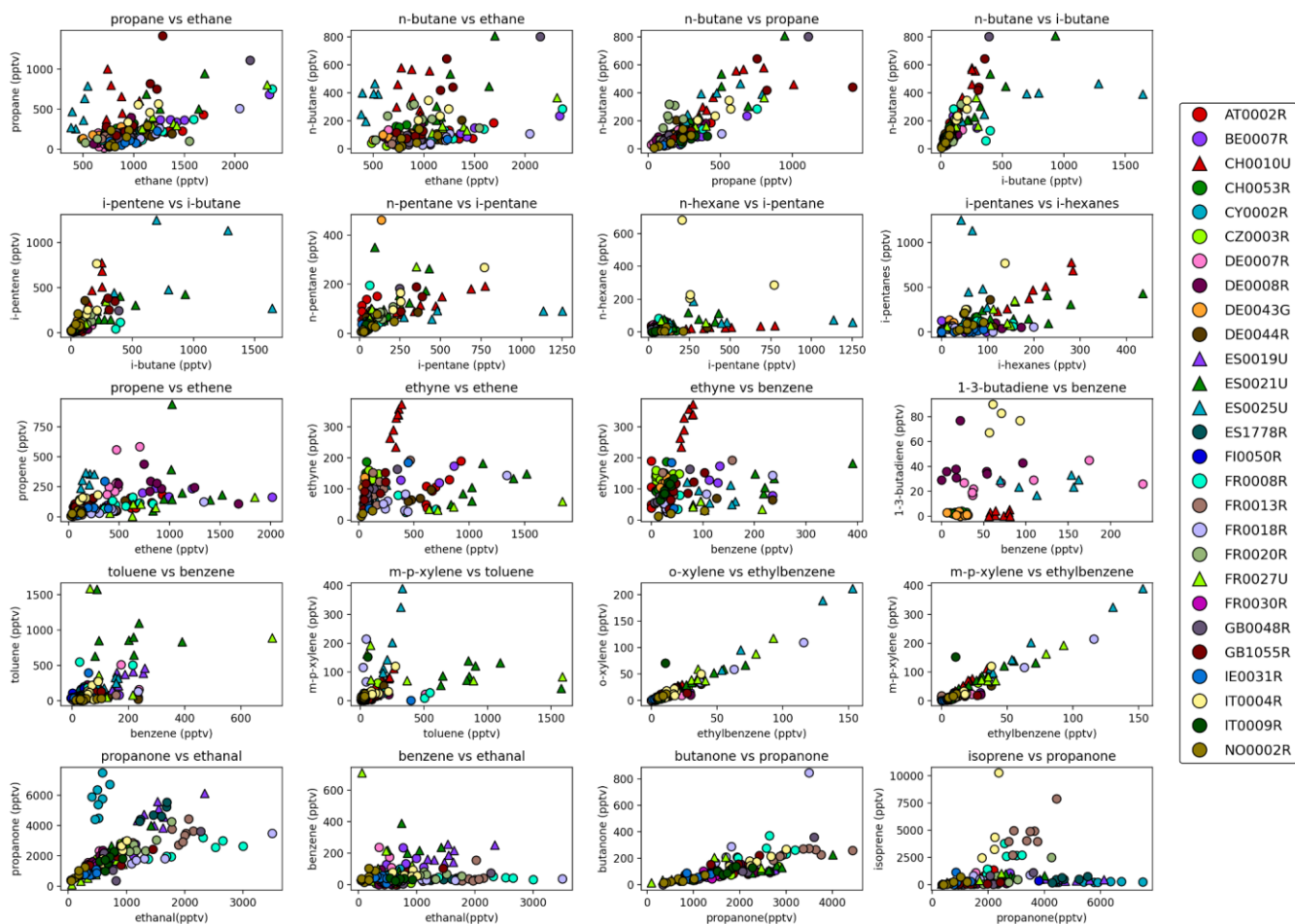


Figure S6. Scatter plots for various VOCs at the different sites. Each marker corresponds to one day during 12-19 July 2022.

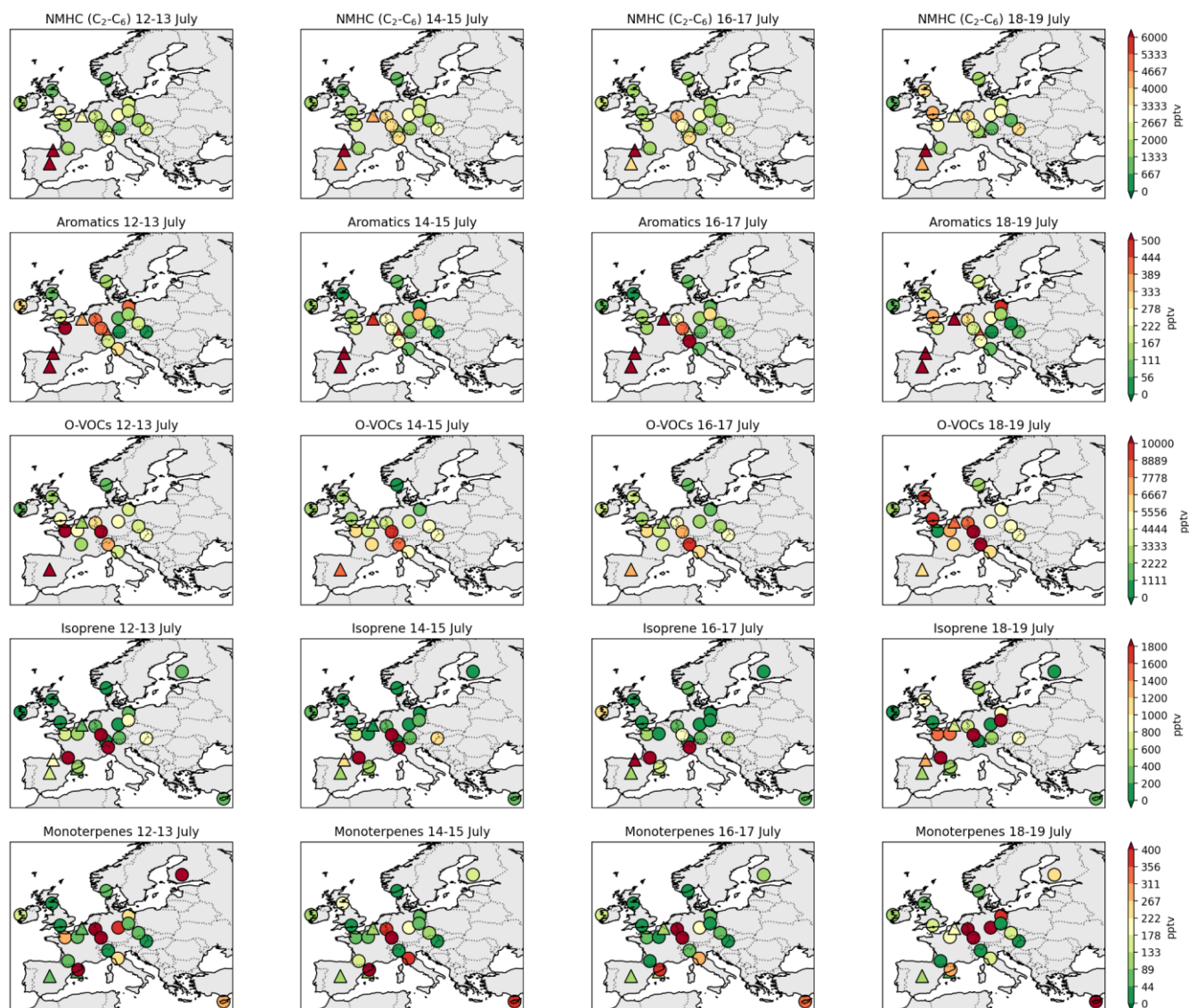


Figure S7. Temporal and spatial variations of different VOC groups. The groups sum the average concentrations for all the relevant components for 4 two-days periods from 12-19 July, 2022. Urban sites are marked with triangles. Sites with a PM₁₀ size cut-off are marked with a thicker border than those with a PM_{2.5} cut-off.

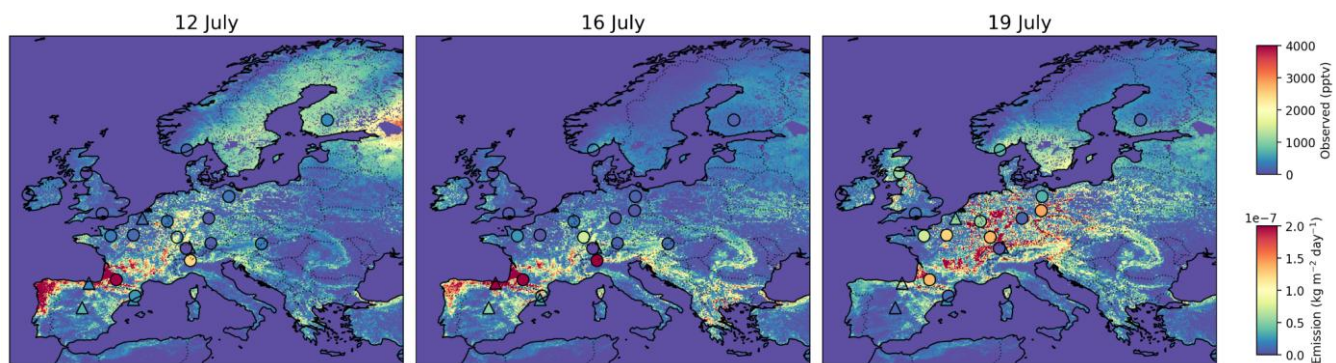


Figure S8. Total daily isoprene emissions (from Hamer et al., 2025) superimposed with observed average isoprene concentrations between 12-16 UTC during the IMP week (12-19 July 2022).

Daily isoprene observations vs emissions, 12-19 July 2022

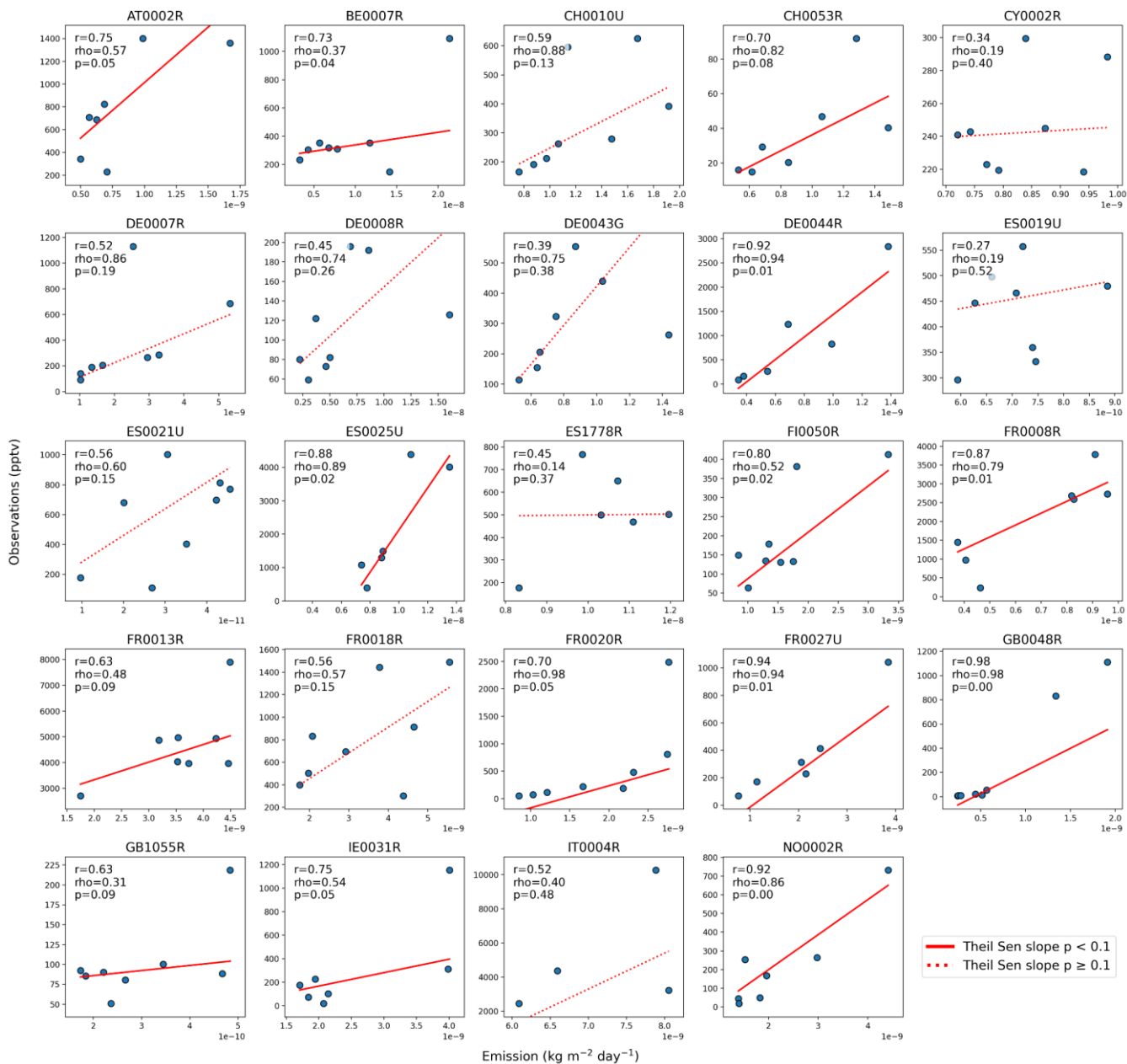


Figure S9. Total daily isoprene emissions from Hamer et al. (2025) compared with the observed average isoprene concentrations between 12-16 UTC during the IMP week (12-19 July 2022). The pearson (r), spearman (ρ) correlations and the p -values are given, and the Theil-Sen slopes are defined with a significant level of $p < 0.1$ (90%).

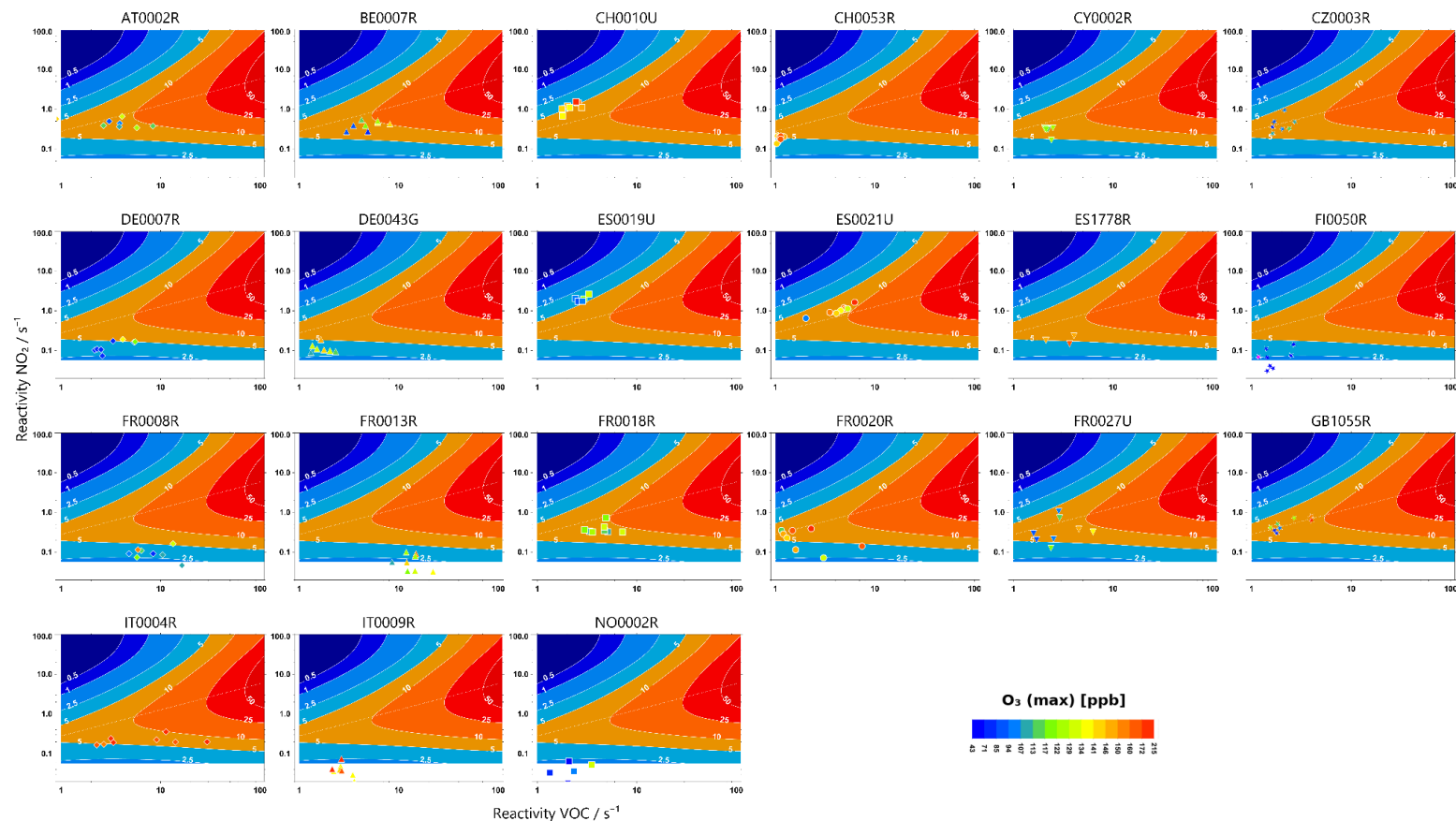


Figure S10. Local ozone production rate (ppb /h) as a function of VOC and NO₂ expressed by their reactivity versus OH radicals (R VOC and R NO₂) and the daily maximum ozone concentrations (ppb) marked in color code and compared to the production rate in the background isoplots based on measurements in Stuttgart in 2020 using the MCM-3.3.1 box model (Ehlers et al., 2016). The dotted line separates the VOC (above the line) and NO_x (below the line) limited regimes of ozone production. At sites without CO and CH₄ data 0.9 s⁻¹ was added to the k_{OH} for the VOC

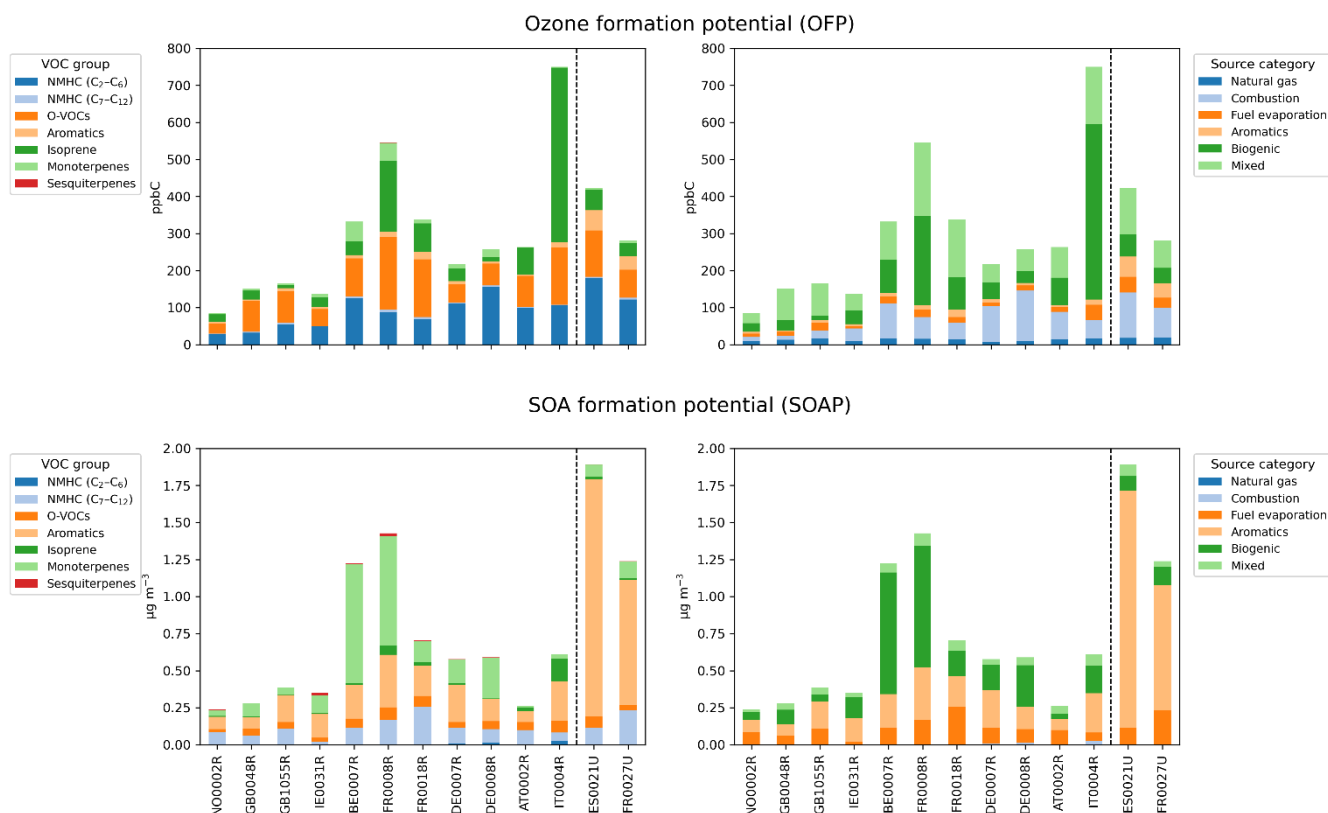


Figure S11. The ozone and SOA formation potentials related to 1) the sum of VOCs in the different component groups (left figures), averaged over 12-16 UTC, 12-19 July 2022 and 2) to the main emission source categories, the VOCs. Natural gas includes propane and ethane. Fuel evaporation covers branched/normal alkanes in the gasoline/distillate range (C₄-C₁₂). Combustion includes unsaturated light hydrocarbons (butenes, pentenes, hexenes, 1,3-butadiene), acetylene, and propene. Aromatics are grouped together (toluene, xylenes, ethylbenzene, trimethylbenzenes, styrene, benzene) since they come from combustion, solvent use, and fuel evaporation. Biogenic includes isoprene mono- and sesquiterpenes Mixed is used for O-VOCs because they're largely secondary with multiple precursors/sources.

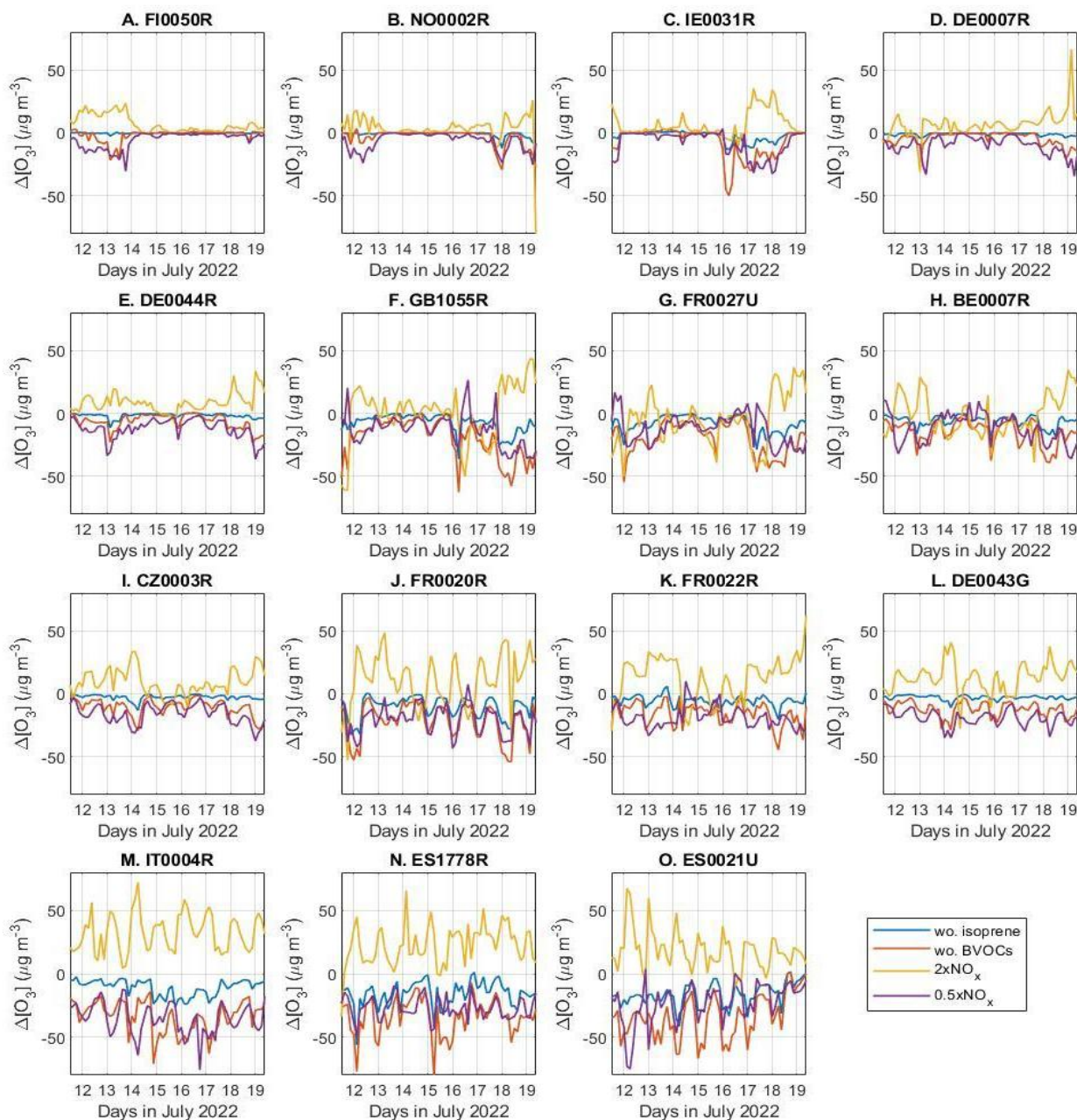


Figure S12. Modelled changes in surface ozone concentration relative to the basecase simulations for four different model sensitivity tests: without biogenic terrestrial isoprene emissions (wo. isoprene), without terrestrial BVOC emissions (wo. BVOCs), with twice the level of anthropogenic NO_x emissions (2xNO_x) and with 50% lower anthropogenic NO_x emissions (0.5xNO_x).

68 **Table S3. Measured and modelled ozone concentrations by the ADCHEM model during the 8-day measurement campaign from**
69 **July 12 to July 19, 2022. r: Pearson correlation coefficients NMB: normalized mean biases, FAC2: fraction of model data points**
70 **that are within a factor of 2 from the measured values**

Station & case	Measured mean [O ₃] (ppbv)	Modelled mean [O ₃] (ppbv)	NMB (%)	<i>r</i>	FAC2
BE0007R					
basecase	42.5	40.8	-2.0	0.80	0.94
wo. isoprene		37.8	-9.3	0.81	0.94
wo. BVOCs		33.4	-19.7	0.80	0.92
2xNO _x		40.2	-4.5	0.74	0.92
0.5xNO _x		34.9	-16.1	0.81	0.94
CZ0003R					
basecase	38.8	41.2	7.7	0.74	0.97
wo. isoprene		39.9	4.4	0.74	0.98
wo. BVOCs		36.0	-6.1	0.73	0.98
2xNO _x		45.9	19.1	0.75	0.93
0.5xNO _x		33.3	-13.1	0.72	0.98
DE0007R					
basecase	32.6	29.4	-5.8	0.60	0.85
wo. isoprene		29.0	-7.0	0.59	0.87
wo. BVOCs		27.3	-12.1	0.60	0.90
2xNO _x		31.8	2.8	0.57	0.86
0.5xNO _x		25.3	-21.2	0.62	0.86
DE0043G					
basecase	55.4	42.8	-22.1	0.63	0.94
wo. isoprene		41.3	-24.8	0.63	0.90
wo. BVOCs		36.6	-33.1	0.61	0.87
2xNO _x		49.2	-10.6	0.70	0.97
0.5xNO _x		33.1	-40.1	0.59	0.77
DE0044R					
basecase		34.9			
wo. isoprene		34.1			
wo. BVOCs		31.7			
2xNO _x		39.3			
0.5xNO _x		29.0			
ES0021U					
basecase	58.2	57.4	-0.8	0.63	0.88
wo. isoprene		49.1	-14.5	0.59	0.82
wo. BVOCs		40.3	-29.0	0.49	0.69
2xNO _x		66.6	14.2	0.62	0.87
0.5xNO _x		45.9	-20.1	0.64	0.79
ES1778R					
basecase	61.2	58.8	-4.2	0.42	0.98
wo. isoprene		50.5	-16.6	0.48	0.97
wo. BVOCs		41.4	-30.4	0.39	0.83
2xNO _x		70.7	14.4	0.57	1.00
0.5xNO _x		45.3	-25.0	0.32	0.89

FI00050R basecase wo. isoprene wo. BVOCs 2xNO _x 0.5xNO _x	21.8	18.4 18.4 17.5 22.0 15.6	-15.9 -16.1 -19.9 0.6 -28.5	0.33 0.33 0.26 0.45 0.16	0.94 0.94 0.94 0.98 0.84
FR0020R basecase wo. isoprene wo. BVOCs 2xNO _x 0.5xNO _x	51.3	50.9 45.8 40.2 56.8 40.5	-1.8 -10.8 -20.8 10.1 -20.6	0.62 0.60 0.54 0.75 0.55	0.97 0.98 0.97 0.90 0.94
FR0022R basecase wo. isoprene wo. BVOCs 2xNO _x 0.5xNO _x	49.1	45.8 43.0 38.2 52.3 36.2	-5.8 -11.3 -20.5 7.0 -25.5	0.71 0.72 0.69 0.69 0.72	1.00 1.00 0.97 0.95 0.98
FR0027U basecase wo. isoprene wo. BVOCs 2xNO _x 0.5xNO _x	38.9	46.9 42.9 36.9 44.4 40.7	20.7 10.5 -4.6 15.2 4.7	0.68 0.68 0.67 0.74 0.67	0.90 0.90 0.92 0.90 0.92
GB1055R basecase wo. isoprene wo. BVOCs 2xNO _x 0.5xNO _x	38.8	42.5 38.9 32.6 43.0 35.9	9.6 0.2 -16.1 10.9 -7.4	0.54 0.53 0.49 0.72 0.34	0.88 0.88 0.89 0.89 0.86
IE0031R basecase wo. isoprene wo. BVOCs 2xNO _x 0.5xNO _x	33.7	26.4 25.3 22.6 29.3 22.3	-22.2 -25.6 -33.5 -12.7 -34.2	0.88 0.89 0.92 0.90 0.86	0.61 0.64 0.63 0.78 0.55
IT0004R basecase wo. isoprene wo. BVOCs 2xNO _x 0.5xNO _x	48.0	76.9 71.4 60.0 93.3 59.0	55.1 44.1 21.6 86.8 18.9	0.71 0.70 0.63 0.74 0.69	0.57 0.61 0.69 0.47 0.67
NO0002R basecase wo. isoprene wo. BVOCs 2xNO _x 0.5xNO _x	32.1	26.9 25.5 25.0 28.6 23.7	-15.0 -15.7 -20.4 -9.6 -24.7	0.52 0.50 0.48 0.44 0.51	0.75 0.77 0.77 0.86 0.71

71

72

73

74

Table S4. Measured and modelled NO₂ concentrations during the 8-day measurement campaign from July 12 to July 19, 2022. *r*: Pearson correlation coefficients NMB: normalized mean biases, FAC2: fraction of model data points that are within a factor of 2 from the measured values

Station & case	Measured NO ₂ (ppbv)	Modelled NO ₂ (ppbv)	NMB (%)	<i>r</i>	FAC2
BE0007R	5.32	4.90	-7.8	0.19	0.79
CZ0003R		2.75			
DE0007R	0.96	1.24	21.9	0.89	0.83
DE0043G	0.82	1.87	124.9	0.42	0.42
DE0044R		2.11			
ES0021U	0.40	12.13	2764.2	0.11	0.0
ES1778R		2.72			
FR0020R		5.31			
FR0022R	1.01	1.79	73.6	0.72	0.67
FR0027U	4.83	6.76	38.9	0.30	0.51
FI00050R	0.46	0.41	-11.7	0.78	0.68
GB1055R	3.66	4.64	22.4	0.37	0.67
IE0031R		0.41			
IT0004R	4.55 ^a	4.99	27.7	-0.24	0.71
NO0002R	0.24	0.36			

75

^aThe measurement data coverage was only 22%.

76

77

Table S5. Measured and modelled OC during the 8-day measurement campaign from July 12 to July 19, 2022.

Station & case	Measured OC in PM _{2.5} (µgC m ⁻³)	Measured OC in PM ₁₀ (µgC m ⁻³)	Modelled OC in PM _{2.5} (µgC m ⁻³)	Modelled OC in PM ₁₀ (µgC m ⁻³)
BE0007R basecase wo. isoprene wo. BVOCs 2xNO _x 0.5xNO _x	1.89		1.584 1.553 1.330 1.418 1.654	1.614 1.582 1.356 1.502 1.692
CZ0003R basecase wo. isoprene wo. BVOCs 2xNO _x 0.5xNO _x	2.64		1.289 1.273 1.086 1.238 1.326	1.308 1.291 1.101 1.255 1.351
DE0007R basecase wo. isoprene wo. BVOCs 2xNO _x 0.5xNO _x	1.76		0.684 0.680 0.589 0.649 0.720	0.706 0.703 0.609 0.672 0.743
DE0043G basecase wo. isoprene wo. BVOCs 2xNO _x 0.5xNO _x			1.372 1.340 1.037 1.274 1.407	1.392 1.358 1.053 1.293 1.432
DE0044R basecase wo. isoprene wo. BVOCs 2xNO _x 0.5xNO _x	2.08		0.786 0.781 0.681 0.740 0.815	0.809 0.804 0.702 0.761 0.839
ES0021U basecase wo. isoprene wo. BVOCs 2xNO _x 0.5xNO _x		5.84	2.322 2.193 1.844 2.207 2.384	2.390 2.254 1.899 2.274 2.455
ES1778R basecase wo. isoprene wo. BVOCs 2xNO _x 0.5xNO _x		3.74	2.153 2.050 1.476 1.926 2.277	2.212 2.096 1.513 1.980 2.344
FI00050R basecase			0.403	0.404

wo. isoprene			0.396	0.398
wo. BVOCs			0.183	0.185
2xNO _x			0.386	0.388
0.5xNO _x			0.408	0.409
FR0020R				
basecase		8.09	1.816	1.857
wo. isoprene			1.770	1.808
wo. BVOCs			1.566	1.601
2xNO _x			1.768	1.807
0.5xNO _x			1.871	1.924
FR0022R				
basecase		3.33	1.369	1.395
wo. isoprene			1.303	1.327
wo. BVOCs			1.111	1.133
2xNO _x			1.307	1.333
0.5xNO _x			1.410	1.442
FR0027U				
basecase			1.874	1.920
wo. isoprene			1.838	1.883
wo. BVOCs			1.705	1.747
2xNO _x			1.760	1.805
0.5xNO _x			1.947	2.002
GB1055R				
basecase	4.09		1.486	1.525
wo. isoprene			1.436	1.471
wo. BVOCs			1.304	1.335
2xNO _x			1.418	1.456
0.5xNO _x			1.529	1.571
IE0031R				
basecase			0.480	0.495
wo. isoprene			0.451	0.474
wo. BVOCs			0.381	0.402
2xNO _x			0.470	0.496
0.5xNO _x			0.487	0.510
IT0004R				
basecase	3.05		3.561	3.596
wo. isoprene			3.413	3.446
wo. BVOCs			2.787	2.815
2xNO _x			3.307	3.346
0.5xNO _x			3.627	3.665
NO0002R				
basecase		0.89	0.618	0.636
wo. isoprene			0.613	0.630
wo. BVOCs			0.554	0.569
2xNO _x			0.606	0.625
0.5xNO _x			0.638	0.655

79

80

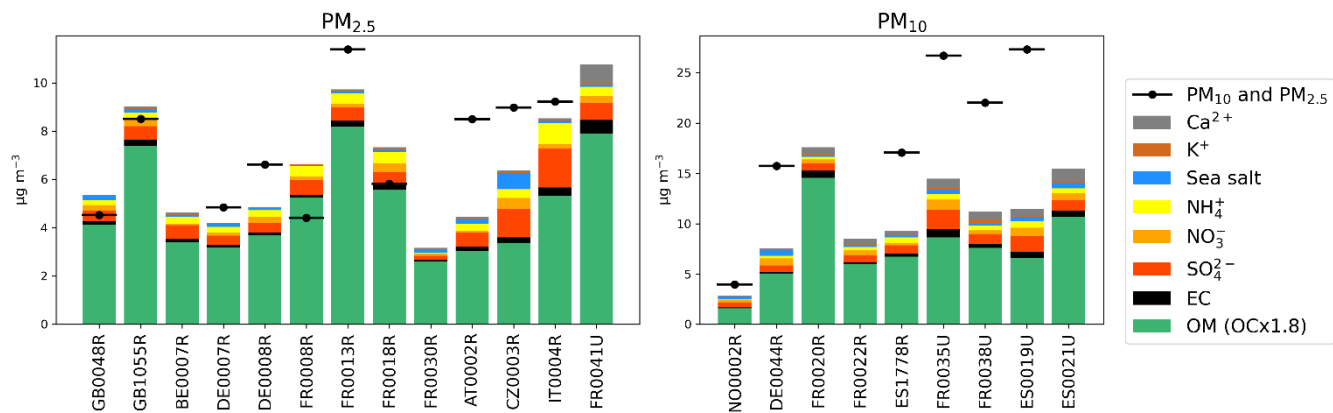


Figure S13. Average chemical speciation and total PM mass concentration (when available) for PM_{2.5} (left) and PM₁₀ (right) for 12-19 July 2022.

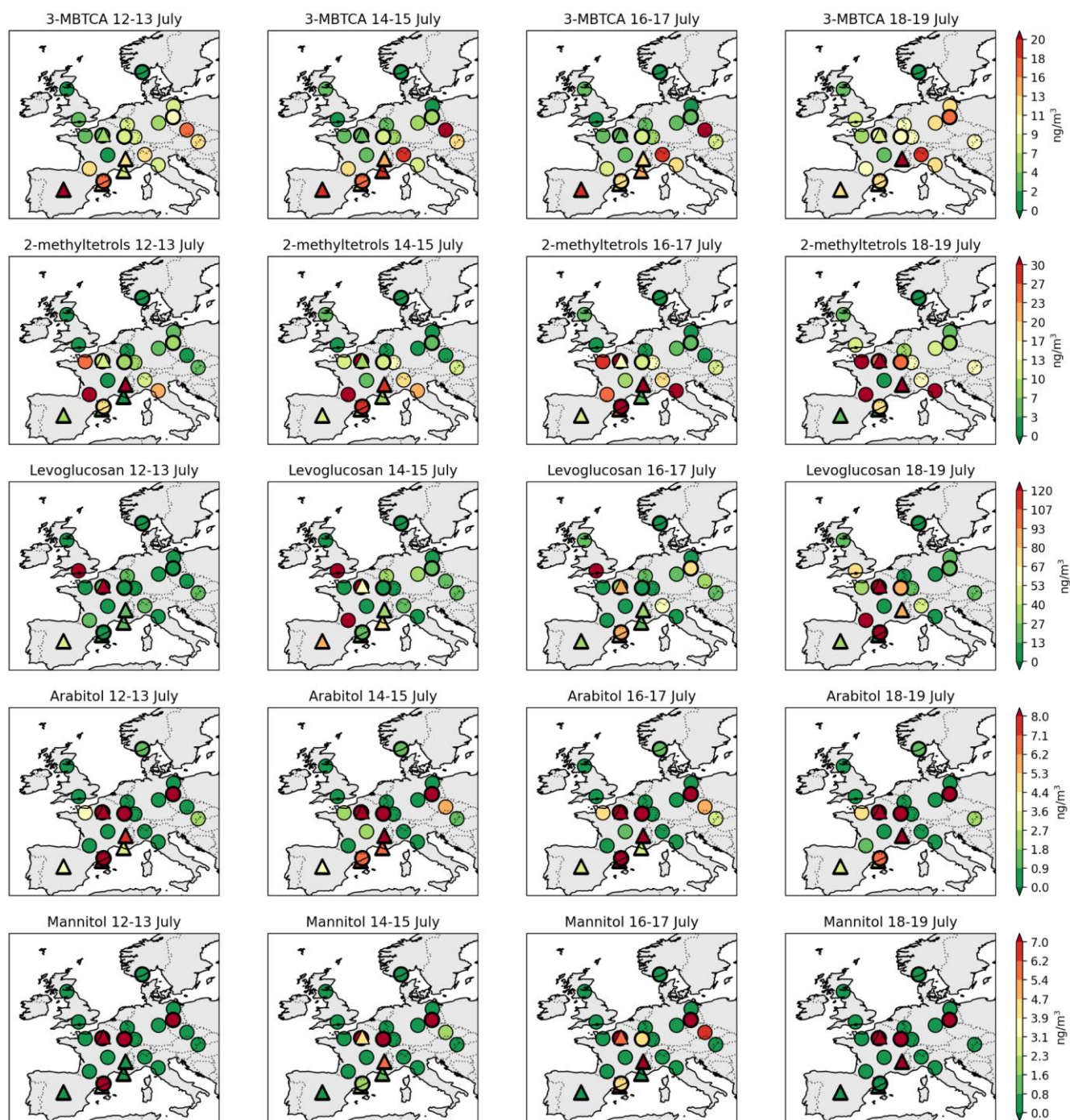


Figure S14. Temporal and spatial variations of different organic tracers. The groups sum the average concentrations for all the relevant components for 4 two-days periods from 12-19 July, 2022. Urban sites are marked with triangles. Sites with a PM₁₀ size cut-off are marked with a thicker border than those with a PM_{2.5} cut-off.

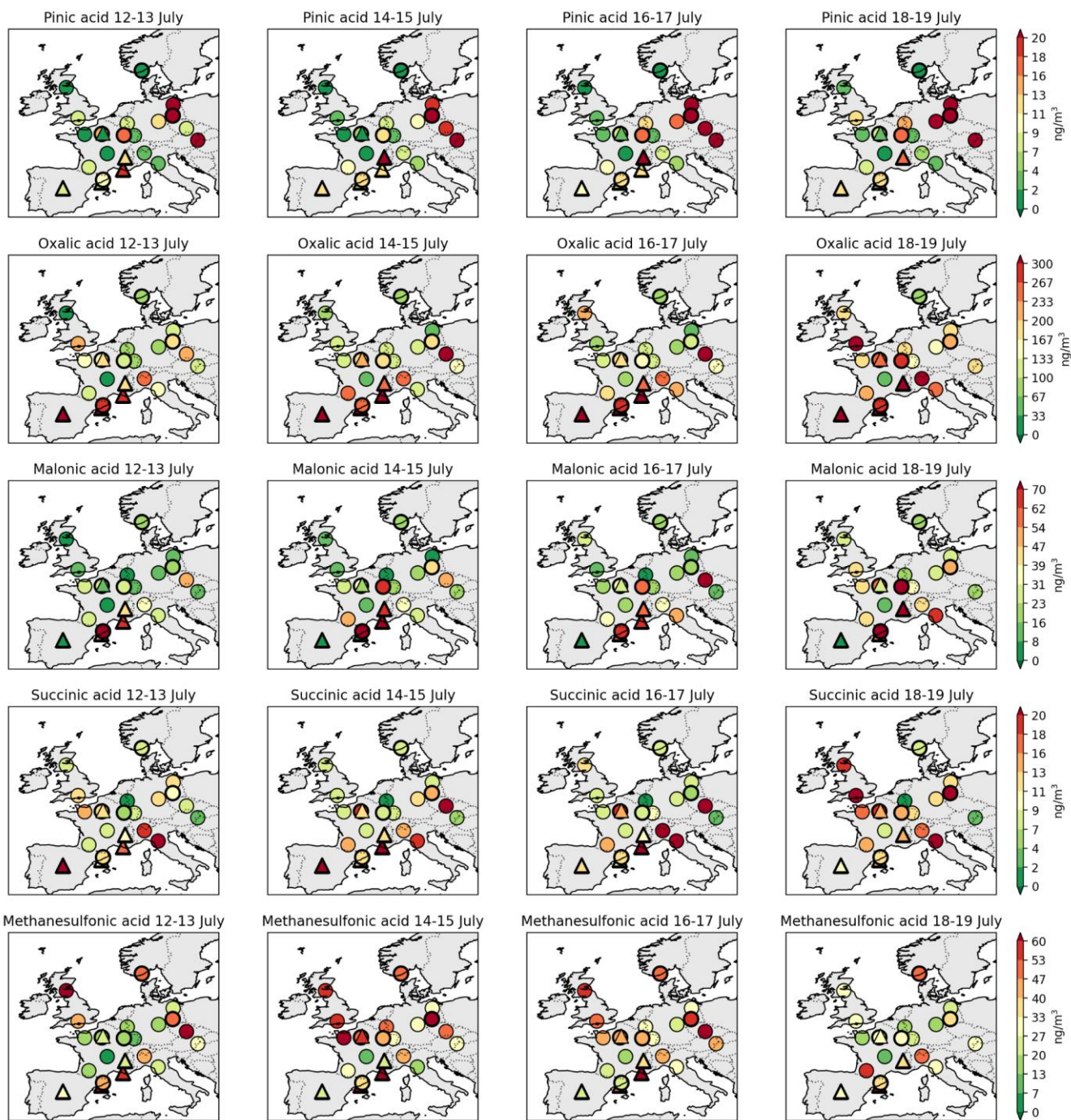
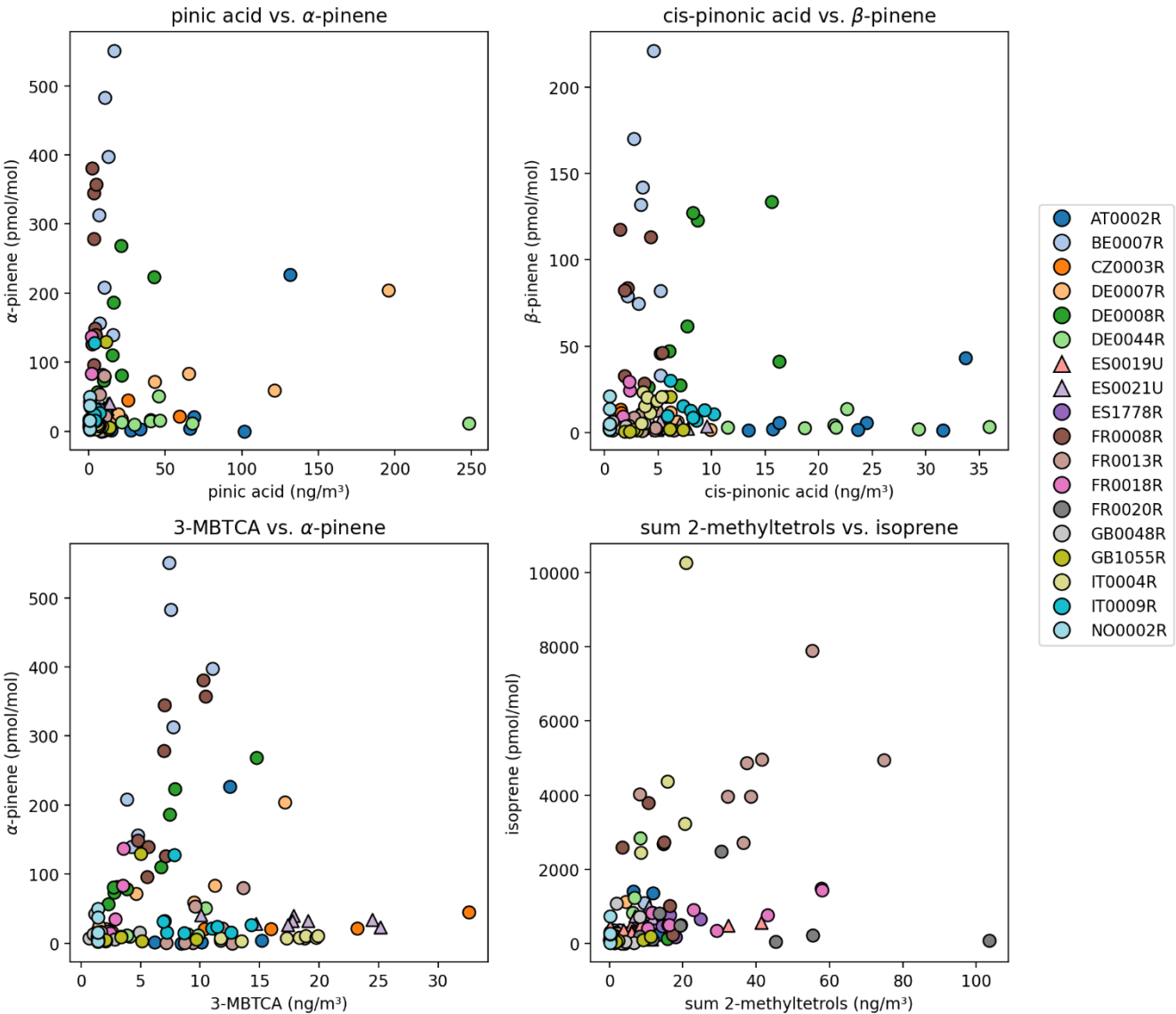


Figure S15. Spatial and temporal distribution of different organic acids. Urban sites are denoted with a triangle. Sites with a PM₁₀ size cut-off are marked with a thicker border than those with a PM_{2.5} cut-off.



93

94 **Figure S16. Scatter plots of selected BVOCs and some of their expected oxidation products. Each marker indicates one day during**
95 **12-19 July 2022. Note that the organic tracer (x-axis) is a 24-hour sample, whereas the selected BVOCs (y-axis) come from samples**
96 **taken between 12-16 UTC over a period of 2 to 4 hours.**

97
98
99
100
101

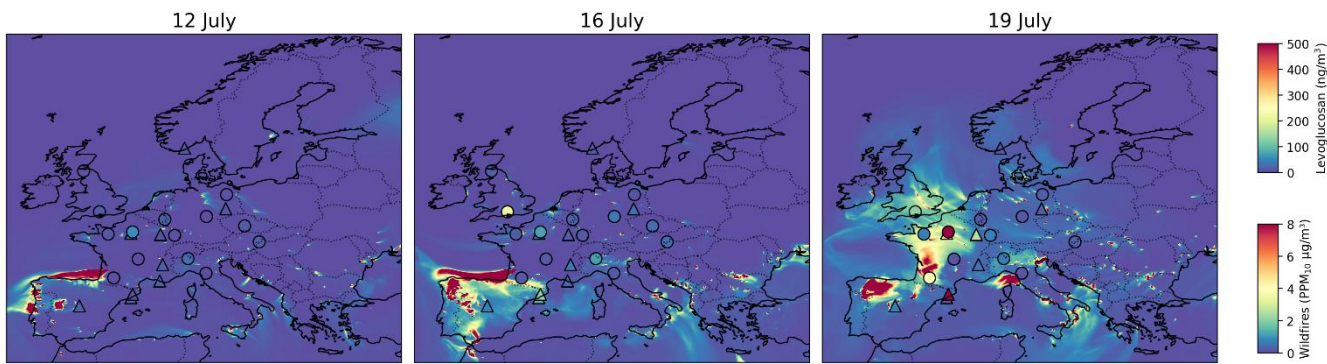


Figure S17. Daily average concentrations of primary PM₁₀ (PPM₁₀) from wildfires calculated with the EMEP model, overlaid with observed levoglucosan concentrations for 12, 16, and 19 July 2022. Sites with a PM₁₀ cutoff are shown as triangles, while those with PM_{2.5} are shown as circles.

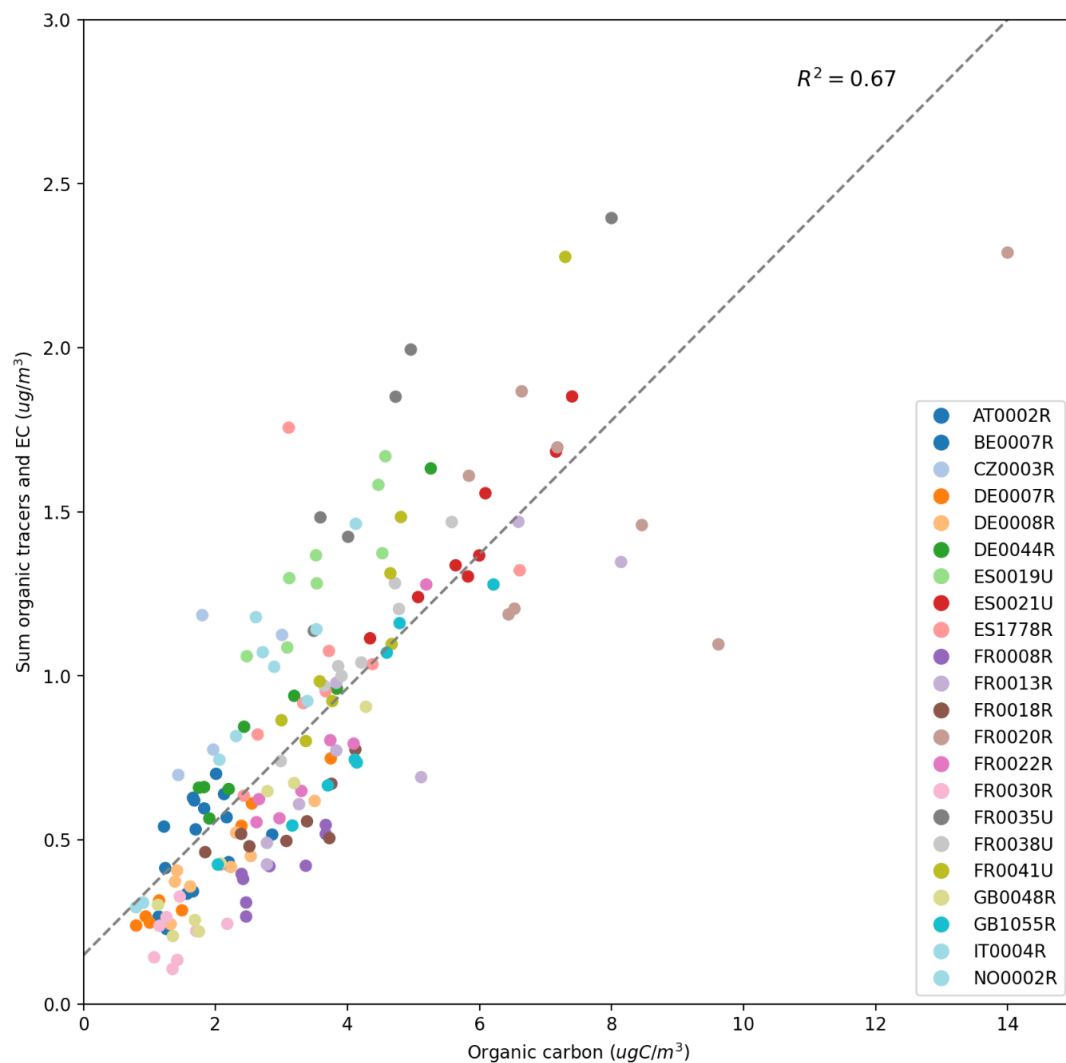


Figure S18. Sum of all tracer concentrations and EC for each sample vs. the OC concentration in the same sample.

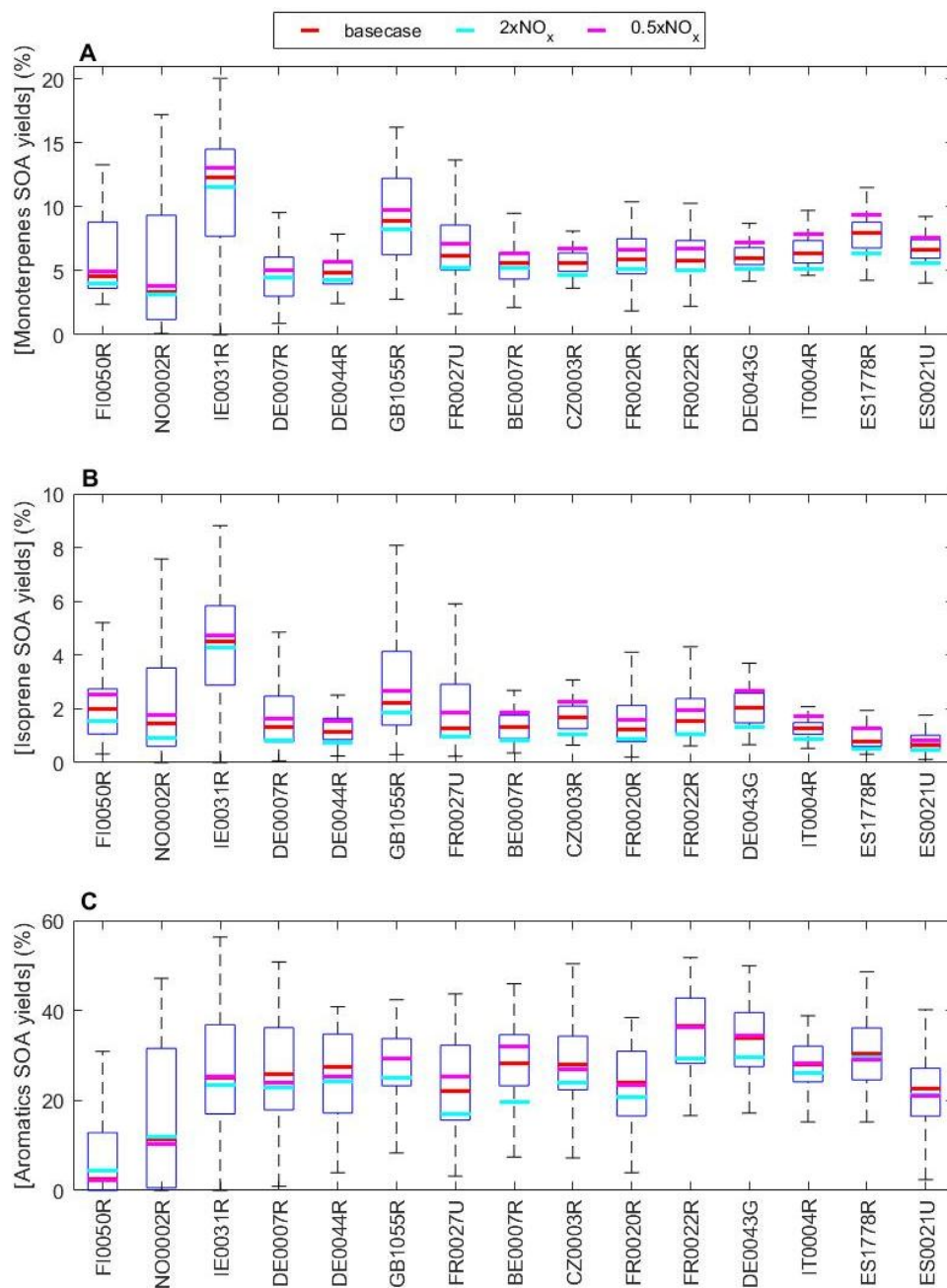


Figure S19. Modelled 10-day cumulative SOA mass yields along the simulated air mass trajectories for (A) monoterpenes (α -pinene, β -pinene, 3-carene, limonene), (B) isoprene and (C) the relatively short-lived aromatic compounds (toluene, xylenes (*m*-xylene, *p*-xylene, *o*-xylene) and phenols (phenol, cresol, 2,4-xyleneol, 2,3-xyleneol, 2,5-xyleneol)). SOA mass yields were calculated as the ratio of the SOA mass formed by condensation in the lowermost 2,100 m of the atmosphere to the total cumulative SOA precursor emissions along the air mass trajectories. The boxes represent the 25-75 percentiles of the modelled (basecase) SOA yields at the different stations. Shown are also the yields with anthropogenic NO_x emissions scaled with a factor of 0.5 or 2.0 (0.5xNO_x and 2xNO_x).

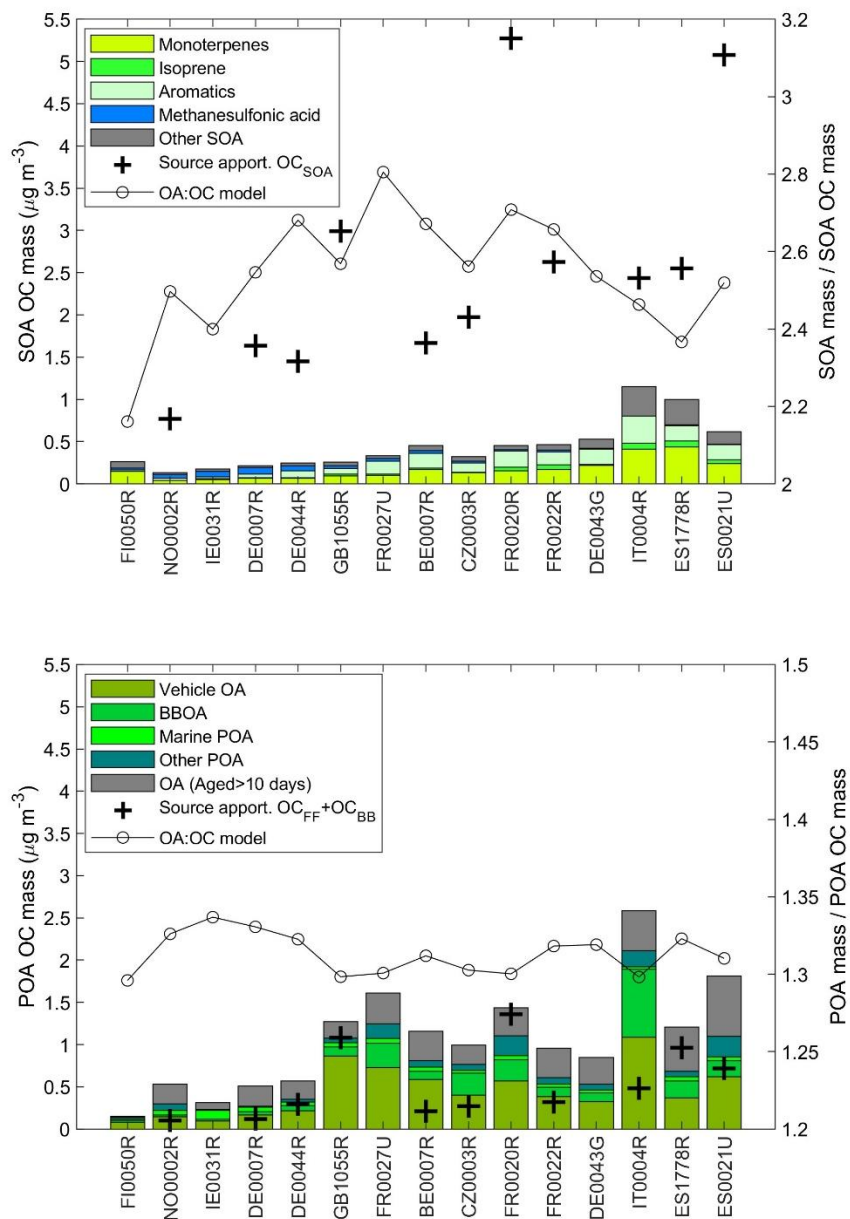


Figure S20. Modelled averaged surface SOA (top panel) and POA (bottom panel) mass concentrations divided into source categories and compared to source apportionment estimates from the tracer method. Solid line indicates the SOA (POA) mass to the SOA (POA) OC mass.

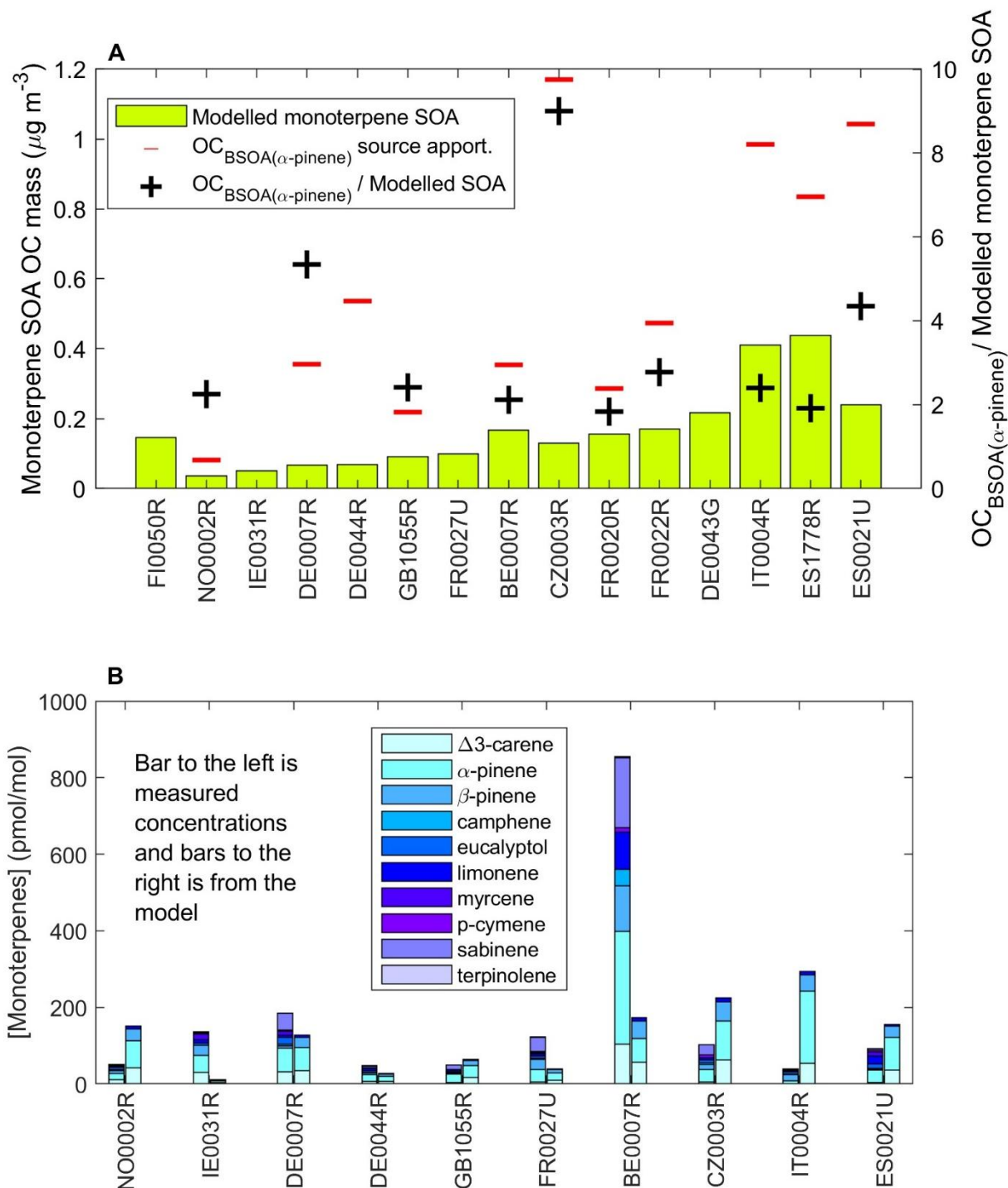
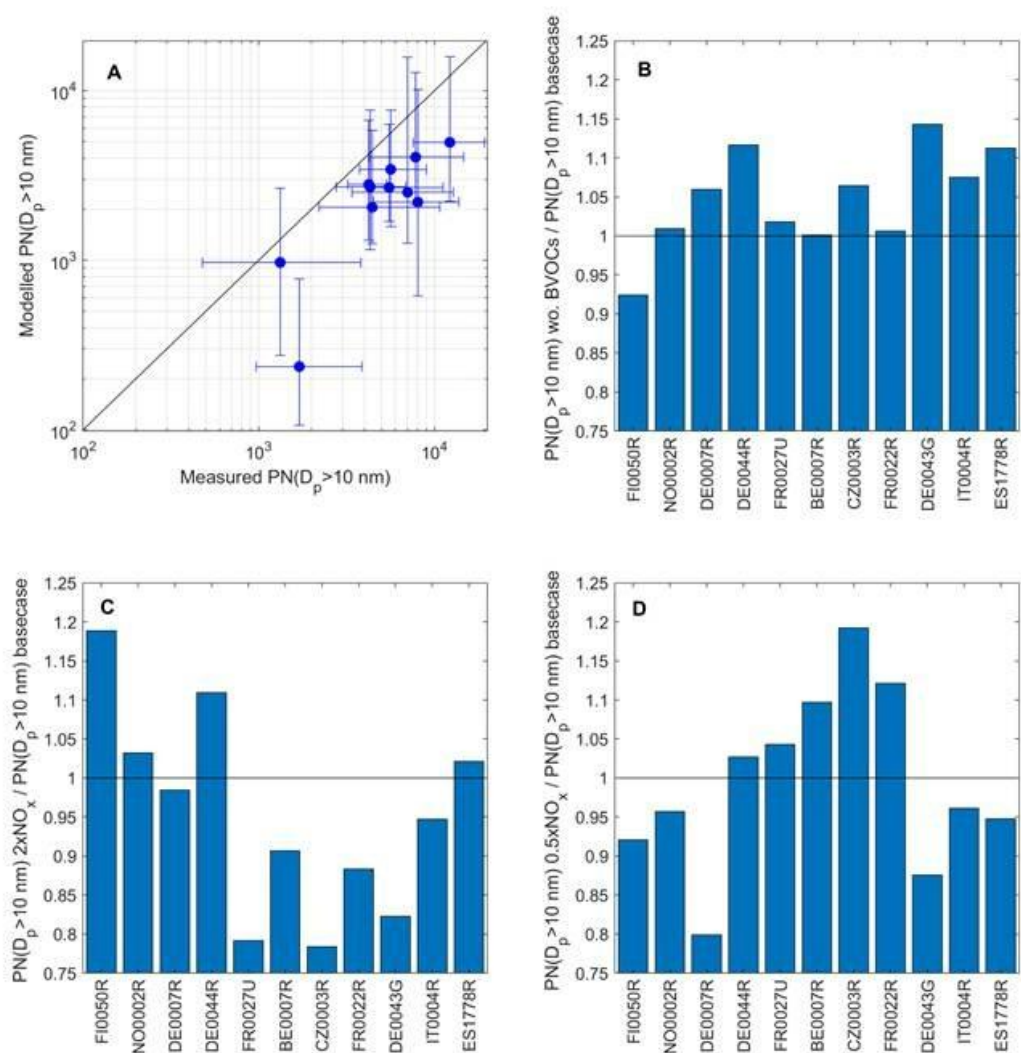


Figure S21. Estimated SOA concentrations from monoterpenes (A, top panel) and concentrations of the individual monoterpenes (B, bottom panel)

120
121



122

123 **Figure S22. Measured and modelled (ADCHEM) number concentrations of submicron particles larger than 10 nm in**
124 **diameter at 11 stations. Panel A – scatter plot with the measured particle number concentrations (PN) on the x-axis**
125 **and modelled PN concentrations on the y-axis. The dots correspond to the median values and the vertical and horizontal**
126 **whiskers in panels A cover the 10-90 percentile ranges of the modelled and measured PN at each station. Panel B-D**
127 **shows the ratio between the median PN from the three sensitivity test simulations (wo. BVOCs, 2xNO_x and 0.5xNO_x)**
128 **and the base case simulations.**

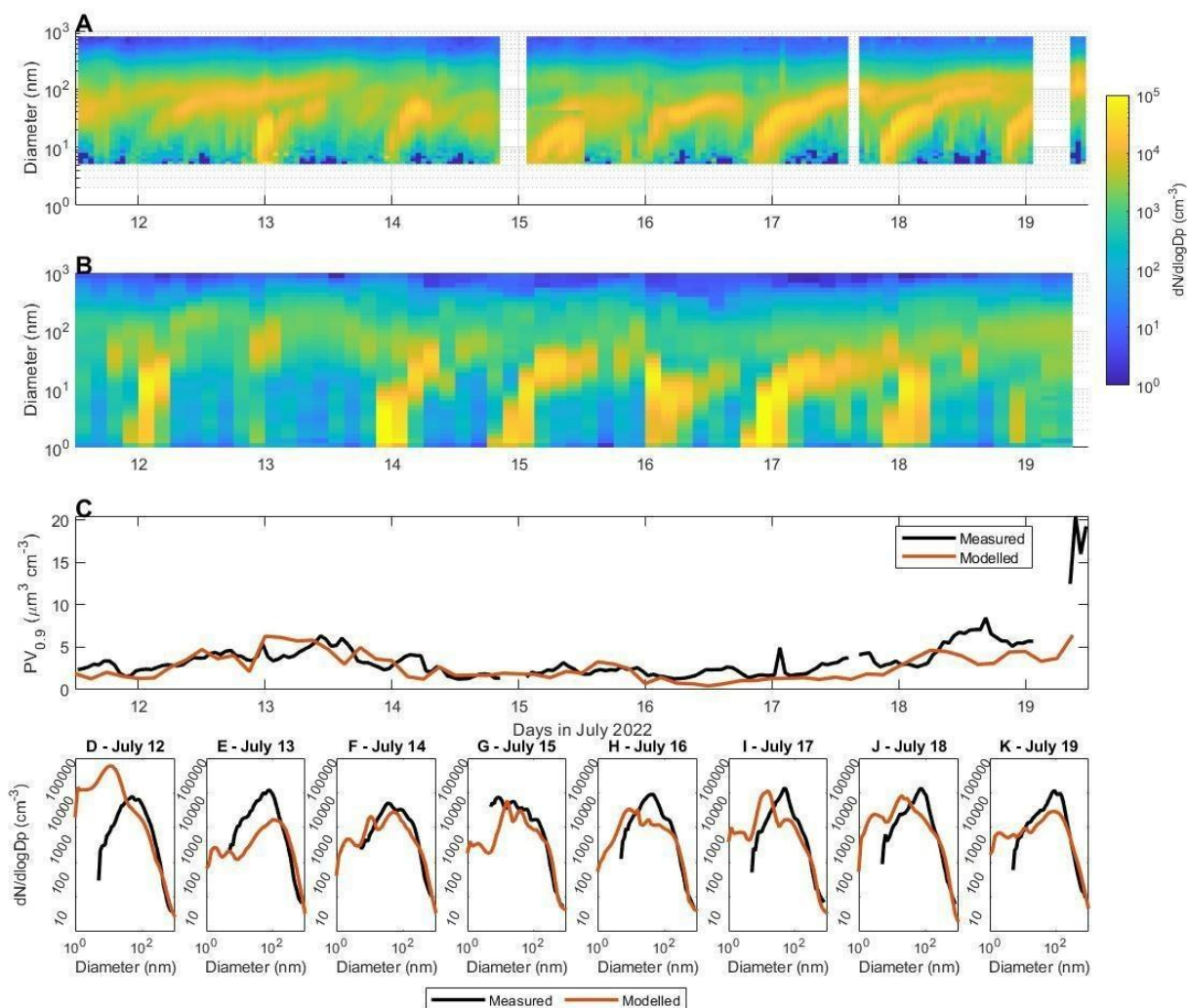


Figure S23. Modelled and measured submicron particle concentrations at Melpitz (DE0044R). Panels A and B show the measured (DMPS) and modelled particle number size distributions, respectively, from July 12 to July 19, 2022. Panel C compares the measured (DMPS) and modelled particle volume concentrations for particles smaller than 0.9 μm in diameter. Panels D to K compare the measured and modelled median particle number size distributions for each campaign day.

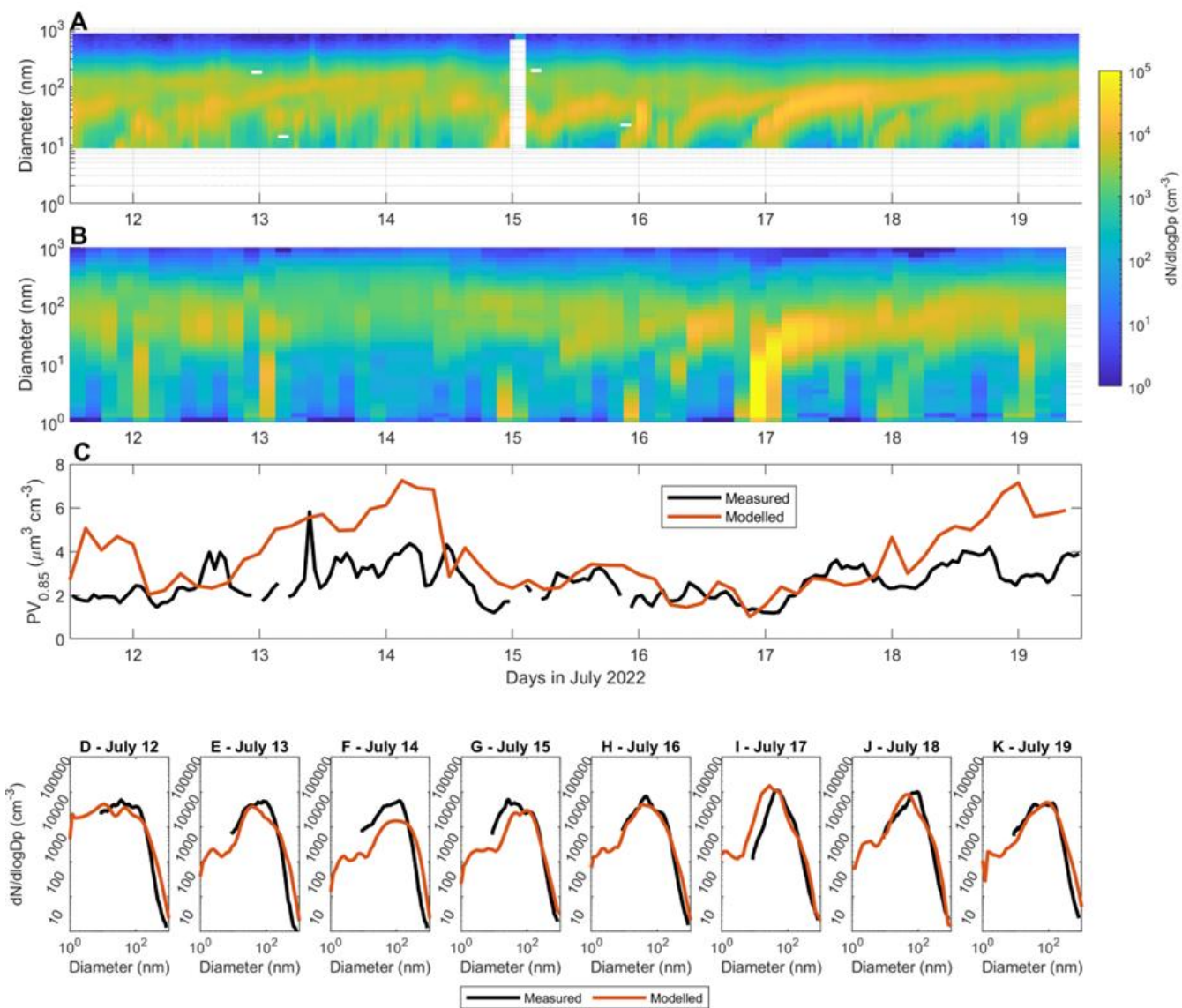


Figure S24. As S23 but for Kosetice (CZ0003R)

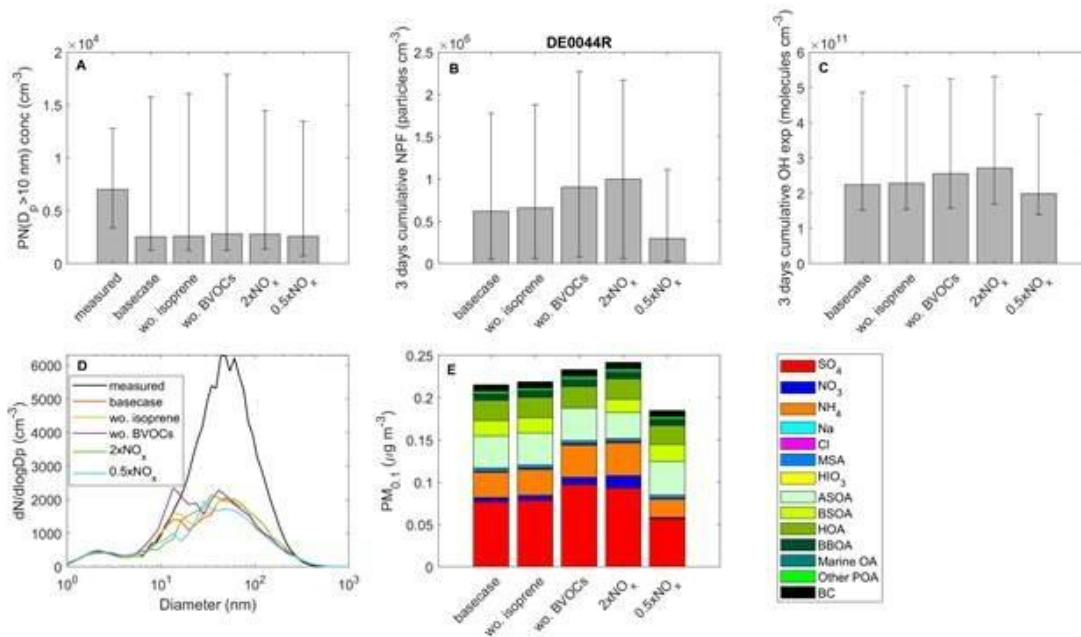


Figure S25. Modelled and measured submicron particle concentrations at Melpitz (DE0044R). The model results are from the ADCHEM base case simulations (basecase), simulations without isoprene emissions (wo. isoprene), without BVOC emissions (wo. BVOCs), and anthropogenic NO_x emissions scaled with a factor of 0.5 or 2.0 (0.5xNO_x and 2xNO_x). Panel A compares the measured and modelled median number concentrations of particles larger than 10 nm in diameter. Panel B shows the modelled cumulative new particle formation (NPF) averaged over the lowest 2,100 m of the atmosphere during the past 3 days upwind the station. Panel C shows the modelled cumulative OH exposure averaged over the lowest 2,100 m of the atmosphere during the past 3 days upwind the station. The measured and modelled median particle number size distributions are compared in panel D. Panel E shows the modelled chemical composition for particles less than 0.1 µm in diameter, i.e. the ultrafine particle (UFP) chemical composition. The whiskers in panels A-C cover the 10-90 percentile range.

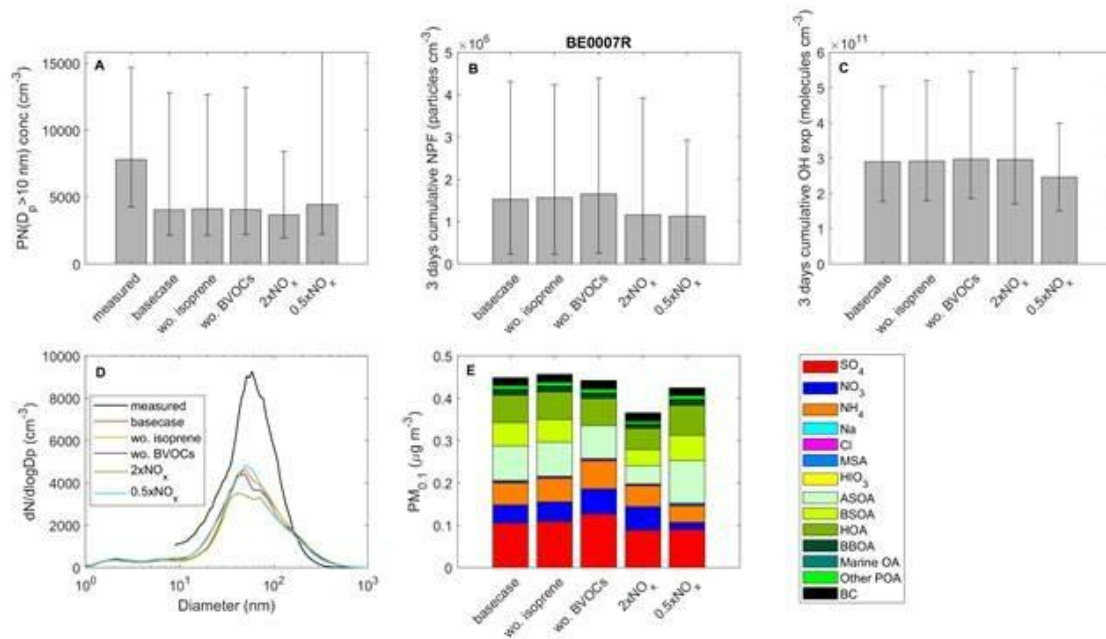


Figure S26. As S25 but for Vielsalm (BE0007R)

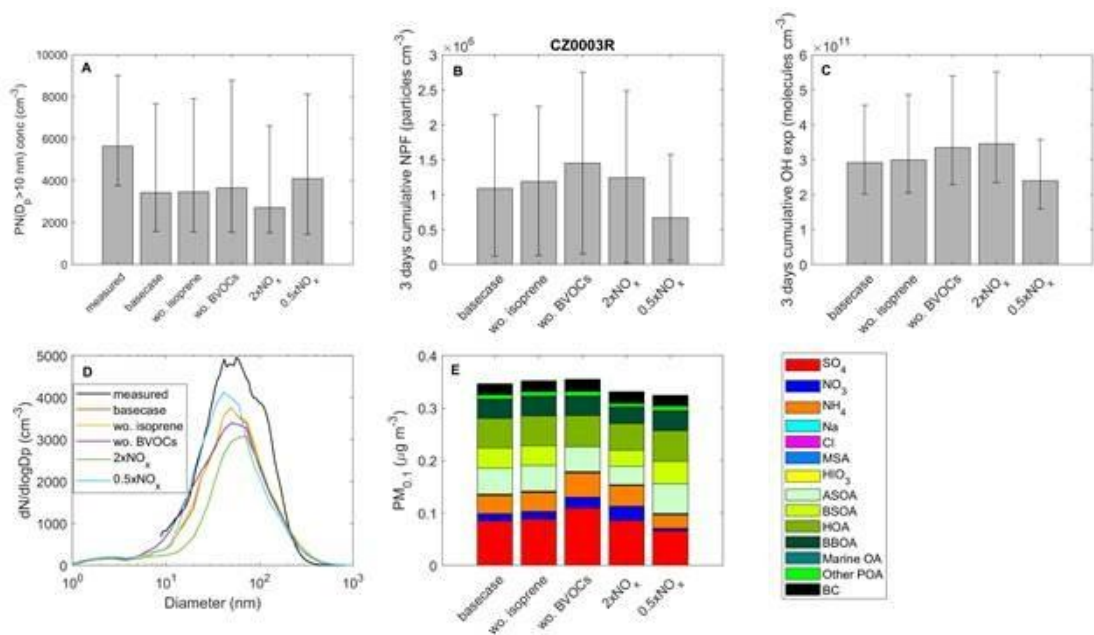


Figure S27. As S25 but for Kosetice (CZ0003R)

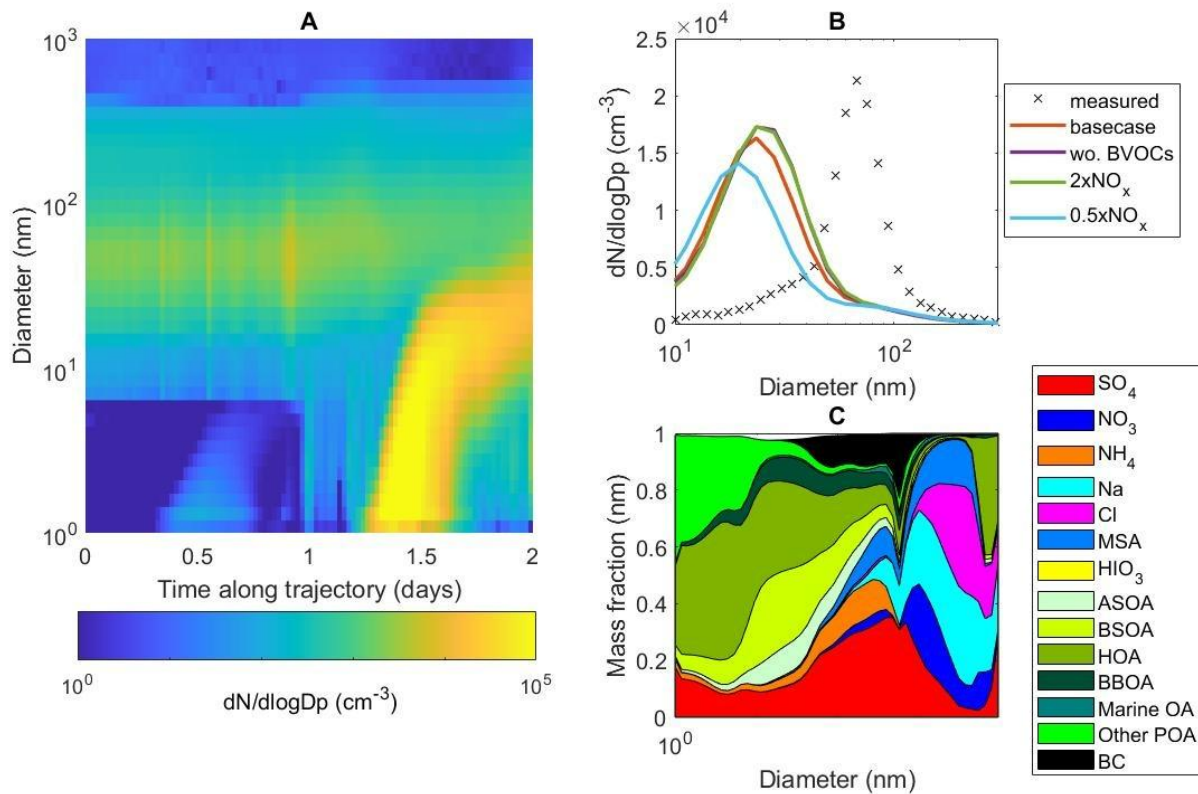
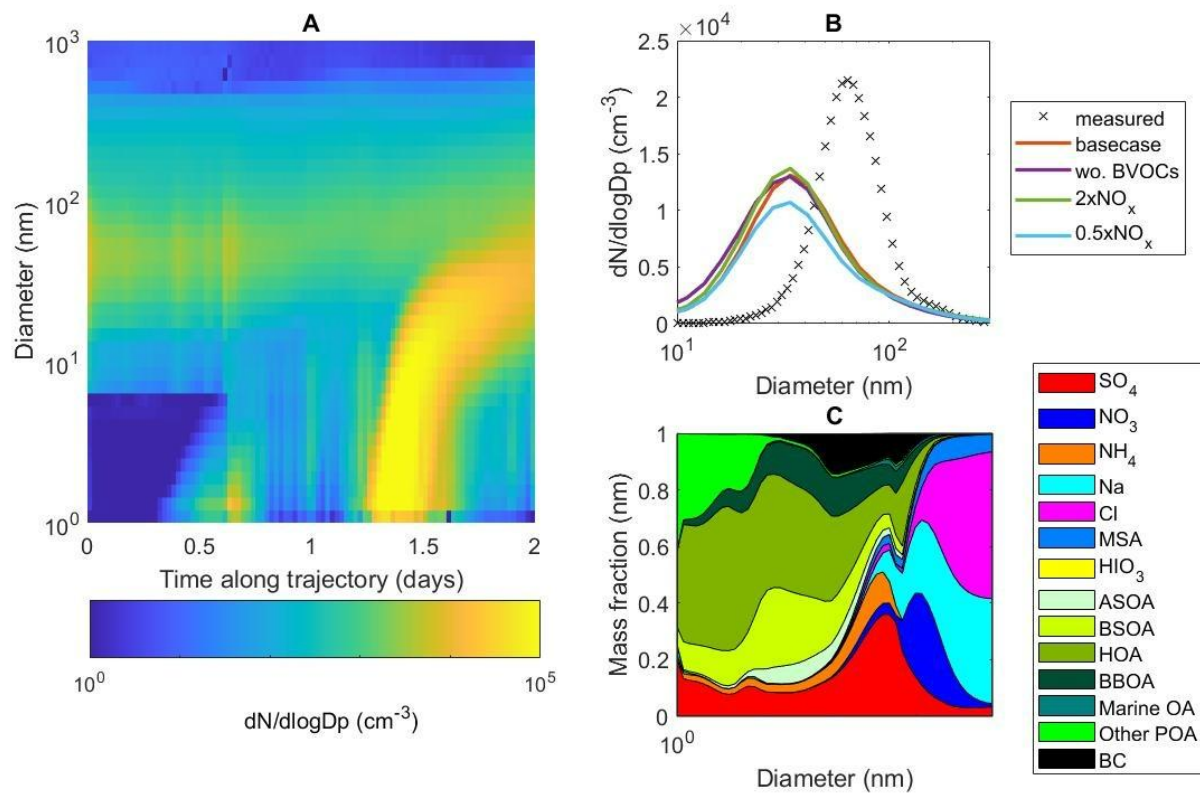


Figure S28. Modelled NPF and particle growth along an air mass trajectory that arrives at Melpitz in the midnight between July 17th and July 18th. Panel A shows the evolution of the modelled particle number size distribution (PNSD) along the air mass trajectory from the basecase model set-up. Panel B compares the measured PNSD at Melpitz at midnight with the modelled PNSD from the basecase, wo. BVOCs, $2x\text{NO}_x$ and $0.5x\text{NO}_x$ model simulations. Panel C shows the modelled size resolved particle chemical composition from the basecase simulation at Melpitz at midnight.



162

163 **Figure S29. Same as S28 but for Kosetice.**

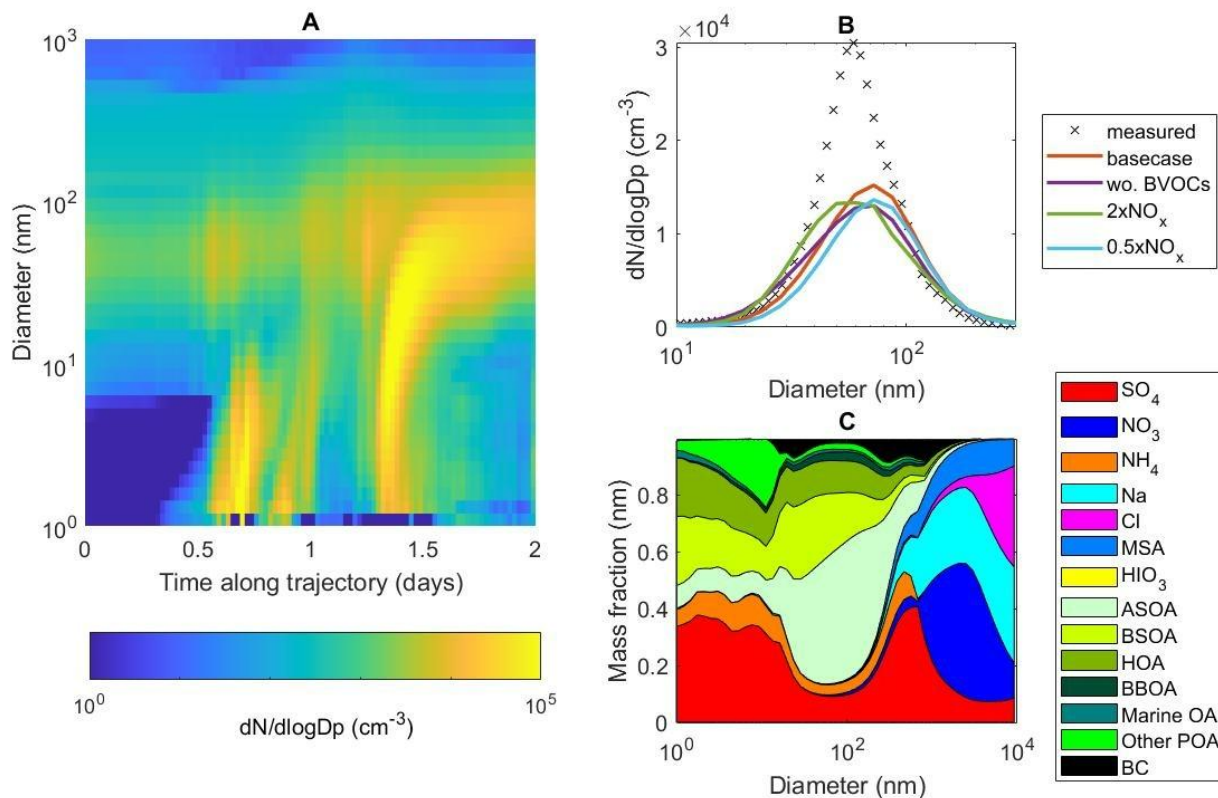


Figure S30. Same as S28 but for Vielsalm.

References

- Ehlers, C., Klemp, D., Rohrer, F., Mihelcic, D., Wegener, R., Kiendler-Scharr, A., and Wahner, A.: Twenty years of ambient observations of nitrogen oxides and specified hydrocarbons in air masses dominated by traffic emissions in Germany, *Faraday Discuss.*, 189, 407–437, <https://doi.org/10.1039/C5FD00180C>, 2016.
- Hamer, P. D., Markelj, M., Rojas-Munoz, O., Bonan, B., Calvet, J.-C., Marécal, V., Guenther, A., Trimmel, H., Vallejo, I., Eckhardt, S., Sousa Santos, G., Sindelarova, K., Simpson, D., Schmidbauer, N., and Tarrasón, L.: Two Biogenic Volatile Organic Compound Emission Datasets over Europe Based on Land Surface Modelling and Satellite Data Assimilation, <https://doi.org/10.5194/essd-2025-442>, 2 October 2025.
- Hersbach, H., Bell, B., Berrisford, P., Biavati, G., Horányi, A., Muñoz Sabater, J., Nicolas, J., Peubey, C., Radu, R., Rozum, I., Schepers, D., Simmons, A., Soci, C., Dee, D., and Thépaut, J.-N.: ERA5 hourly data on single levels from 1940 to present, <https://doi.org/10.24381/CDS.ADBB2D47>, 2023.
- Hjellbrekke, A.-G. and Solberg, S.: Ozone measurements 2022, NILU, Kjeller Norway, 2024.